ORGANIC MATTER REMINERALIZATION IN COASTAL SEDIMENTS IN AND AROUND KANE‘OHE BAY, HAWAI‘I

A DISSERTATION SUBMITTED TO THE GRADUATE DIVISION OF THE UNIVERSITY OF HAWAI‘I AT MĀNOA IN PARTIAL FULFILLMENT OF THE REQUIREMENTS FOR THE DEGREE OF DOCTOR OF PHILOSOPHY IN OCEANOGRAPHY

DECEMBER 2011

By:
Rebecca A. Briggs

Dissertation Committee:
Kathleen Ruttenberg (Chairperson), Brian Glazer, Fred Mackenzie, Margaret McManus, Megan Donahue

Keywords: biogeochemistry, coastal, sediments, redox, organic matter, porewater

"The cure for anything is salt water-sweat, tears, or the sea."

~Isak Dinesen

Acknowledgements

I would like to express my profound gratitude to my PhD advisor Kathleen Ruttenberg, who has been an exceptional role model and motivated me to become a better scientist. I am grateful for her guidance, patience and mentoring throughout my research.

I would also like to thank my thesis committee members, Brian Glazer, Fred Mackenzie, Margaret McManus, and Megan Donahue, for their support and supervision. I am fortunate to have worked with a group of exceptionally talented researchers that were generous with their time and advice, resulting in the success of the research presented in this dissertation.

The opportunity to become involved with the organization Paepae O He'eia, whose members maintain the historical and structural integrity of He'eia Fishpond, has been greatly appreciated. He'eia Fishpond is of cultural importance to the Hawaiian community and I was provided a unique experience in collaborating with the He'eia o'hana. The opportunity to conduct research at the fishpond and get to know the members of the o'hana has deeply impressed in me the importance of cultural understanding and mutual respect between science, tradition, and conservation.

I would also like to give a special thanks to my friends and fellow lab members: Marcie Grabowski, Dan Sulak, Chip Young, Danielle Hull, Jackie Padilla-Gamino, Jillian Ward, Karl Stein, and the numerous other volunteers who helped during fieldwork and within the laboratory making the completion of this study possible. I could not have conducted electrochemical work without the help of In-Chieh Chen and Amanda Ricardo, who spent countless hours polishing electrodes and collecting sediment porewater data.

Thanks are also due to the many others who have contributed indirectly to the success of the scientific work presented in this dissertation. Though the list is much too long to include in this space, without the support and generosity of my colleagues in the scientific community and the administrative staff of the Department of Oceanography and the University of Hawaii Seagrant Office, the research conducted would not have been possible. Within each chapter of this dissertation additional acknowledgements are given to the funding agencies and the people that directly contributed to that body of work.

And, most importantly, I owe my deepest gratitude to my close friends and family who have supported me through this incredible journey. **MAHALO**

Abstract

Nutrient cycles in shallow, near shore environments can be profoundly influenced by sediments, via the burial or release of nutrients through organic matter (OM) remineralization during diagenesis. The decomposition and burial of OM in sediments are key processes influencing biogeochemical cycles of nutrients (nitrogen, phosphorus) and carbon in coastal waters on time scales ranging from seasonal fluctuations to long, geologic timescales. This dissertation examines several aspects of OM remineralization in marine sediments, and addresses fundamental questions that link organic matter source, sediment redox state, and nutrient cycling. The studies described in this dissertation include development of new techniques that permit quantification and characterization of OM sources to marine sediments, which will be informative for OM preservation studies (Chapters 2-3); in the latter portion of this dissertation (Chapters 3-6), particular aspects of early diagenetic pathways of OM remineralization are examined. The studies described herein place constraints on sources and sinks of bioavailable nutrients in coastal sediments, including the flux of nutrients at the sediment-water interface. As such, the processes examined throughout this dissertation are essential to understanding coastal ocean biological productivity, and can shed light on transport of bioavailable nutrients from coastal waters to the open ocean. The research presented here was conducted in and around coastal Kane‘ohe Bay and, as such, reveals processes that may be unique to coastal systems adjacent to new, volcanogenic islands. However, many of the processes studied are more broadly operant, and insights into processes occurring within the coastal sediments of our study site can be readily extrapolated to other coastal systems.

Table of Contents

Acknowledgements iii

Abstract iv

Chapter 1 Introduction 1

1.1 Scope of work 2

1.2 Dissertation research: Method development 3

1.3 Dissertation research: Field experiments 4

Chapter 2 Quantifying organic carbon and nitrogen concentration and isotopic compositions in carbonate-dominated coastal marine sediments 6

Abstract 7

2.1 Introduction 8

2.2 Materials and procedures 10

Sample collection 10

Bulk sediment carbon and nitrogen analyses 10

Bulk sediment phosphorus analysis 13

End member analysis 13

Error estimation 13

2.3 Assessment 15

Carbon and nitrogen concentrations 15

Carbon and nitrogen isotopic composition 16

2.4 Discussion 19

2.5 Comments and recommendations 20

Acknowledgements 21

Chapter 3 Evaluation of novel SEDEX extraction steps for labile organic phosphorus and $CaCO_3$-bound phosphorus in aquatic sediments 22

Abstract 23

3.1 Introduction 24
3.2 Material and methods 26
General strategy 26
Extractants and extraction approach 28
Phosphorus analysis of supernatants 29
3.3 Standardization experiments: Design and procedure 30
Efficiency experiments for L-OP 30
Specificity experiments for L-OP 31
Matrix experiments for L-OP 31
Comparison of SEDEX method with and without Pre-Extraction 32
Combined efficiency-specificity experiments for $CaCO_3$-bound P 32
3.4 Results and discussion 33
3.4.1 Standardization, efficiency, and matrix experiments for L-OP determination 33
Filter durability assessment 33
Pre-Extraction efficiency determinations 33
Pre-Extraction specificity evaluation 34
Evaluation of matrix effects 36
3.4.2 Efficiency and specificity of TAC for $CaCO_3$-bound P 41
3.4.3 Comparison of SEDEX with and without Pre-Extraction 42
L-OP analogue phase results 42
Pre-Extraction followed by SEDEX 43
Phytoplanktonic L-OP extracted in Pre-Extraction and Step I 44
Comparison of SEDEX data from seabed sediments with and without Pre-Extraction 46
3.4.4 Further insight into 'refractory phytoplanktonic-P' 47
Appendix 3.1 Sep-Pak analysis of SEDEX-Step II (CDB) supernatants for quantification of Fe-bound P 49
Appendix-3.2 Miscellaneous analytical details regarding Pre-Extraction 52
Acknowledgements 53

Chapter 4 Linking source, abundance and lability of sedimentary organic matter to remineralization efficiency 54
Abstract 55
4.1 Introduction 56
4.2 Study site 58
4.3 Methods 59
Sample Collection 59
Core processing and analysis 59
Incubation set-up 60
4.4 Estimation of mineralization efficiency 62
Conceptual framework 62
Calculations 63
4.5 Results 65
4.6 Discussion 70
Sources and degradation of OM end members 70
Sources and degradation of OM sediments 72
Quality versus quantity of OM 75
4.7 Conclusions 82
Acknowledgements 85

Chapter 5 Impact of *Montipora capitata* coral spawning events on Hawaiian coastal biogeochemistry 86
Abstract 87
5.1 Introduction 88
5.2 Methods 90
Study Site 90
Instrumentation 90
Coral host tissue and spawn material collection and on-shore processing 91
Coral host tissue and spawn material processing and analysis 91

Water and sediment sample collection 92
Sediment sample processing and analysis 93
Water sample processing and analysis....94
Benthic nutrient efflux calculations....94
5.3 Results....95
Coral spawning and physical conditions 95
Coral host tissue and spawn material....97
Water column and sediment 99
5.4 Discussion 101
Characterization of coral host tissue and spawn material....101
Tracking the impact of SDOM on water column suspended and surface sediment organic matter 103
Water column dissolved nutrient perturbations by SDOM input and phytoplankton response 107
Contribution of SDOM to regional carbon and nitrogen loading....113
Acknowledgements 116

Chapter 6 Diel variations in sediment redox conditions: Impacts on sediment nutrient cycling in a nearshore coastal environment 117
Abstract....118
6.1 Introduction....119
6.2 Objectives and rationale....120
6.3 Background 123
Cycling of dissolved ammonium in coastal sediments....123
Coupled iron and phosphorus in sediment porewaters 124
Dissolved organic phosphorus in sediment porewaters....125
Coupled iron and sulfur cycling in coastal sediments 126
6.4 Study site....127
6.5 Methods....128
Sampling rationale and experimental setup....128

Sample collection....128
Instrumentation....129
Sediment and water sample analysis....129
Profiling of sediment cores....130
6.6 Results....131
Study site background information....131
Porewater profiles....132
6.7 Discussion....134
Biological influence on water column....134
Diurnal trends in sediment porewaters....140
Porewater profiles of NH_4^+....148
Stoichiometric nutrient regeneration....152
The missing P story....153
6.8 Conclusions....156
Acknowledgements....158

Chapter 7 Conclusions....159

References....166

List of Tables

Table 2.1 Method of analysis for carbon and nitrogen concentrations and isotopic compositions and approximate mass used for each analytical procedure.....11

Table 2.2 Carbon and nitrogen concentrations and isotopic compositions of laboratory reference materials.....12

Table 2.3 Carbon and nitrogen concentrations of sediments samples from Kane‘ohe Bay.....14

Table 2.4 $\delta^{13}C$ and $\delta^{15}N$ values for sediment samples from Kane‘ohe Bay.....17

Table 3.1 Analog phases used for Pre-Extraction experiments.....27

Table 3.2 The percentage of P extracted during the Pre-Extraction method from pure minerals phases with surface sorbed P.....36

Table 4.1 Carbon, nitrogen and phosphorus concentrations and isotopic composition of potential end member.....66

Table 4.2 Calculated benthic flux of NH_4^+.....70

Table 4.3 Metabolic rates estimated from whole core incubations.....79

Table 5.1 Results of the general linear model.....97

Table 5.2 Release of carbon and nitrogen from coral eggs during spawning events. 114

Table 6.1 Electrode reactions at the Au/Hg electrode surface 130

Table 6.2 Depth (cm) of disappearance (O_2, Fe^{2+}) and appearance (Fe^{2+}, H_2S) in porewaters 140

List of Figures

Figure 2.1 Nitrogen quantification curve for the Carlo Erba NA 2500 elemental (CN) analyzer 15

Figure 2.2 Sediment organic carbon $\delta^{13}C$ values plotted against molar organic (OC:OP) ratios 19

Figure 3.1 SPExMan-SEDEX scheme with Pre-Extraction and the separation of the combined reactive Ca-P reservoir scheme 25

Figure 3.2 The concentration of P extracted from each step in the Pre-Extraction method for analog plankton phases 34

Figure 3.3 Recovery of OP from the bulk plankton analogue phase in the Pre-Extraction method 35

Figure 3.4 Matrix experiment results 38

Figure 3.5 Plankton analogue phases subjected to the full SEDEX procedure, with and without the Pre-Extraction method 40

Figure 3.6 Dissolution experiments with $CaCO_3$ and CFA mineral phases using triammonium citrate (TAC) 42

Figure 3.7 Percentage of TDP (IP + OP) extracted in Pre-Extraction + Step I, compared to the percentage of TDP extracted in Step I 45

Figure 3.8 Sediment samples subjected to the Pre-Extraction and SPExMan-SEDEX method 46

Figure 3.9 The percentage of P extracted from two types of pure DNA 47

Appendix Figure 3.1 Reusability test on the Sep-Pak cartridges 51

Figure 4.1 Aerial photograph of He'eia Fishpond 58

Figure 4.2 Incubation setup and schematic 61

Figure 4.3 End member box plot of molar OC:TN:OP ratios versus $\delta^{13}C$ 71

Figure 4.4 Sediment OC:TN:OP ratios versus $\delta^{13}C$ 73

Figure 4.5 Down core sediment profiles of OC:TN ratios, OC:OP ratios, and wt% OC 76

Figure 4.6 Down core porewater profiles of NH_4^+ and PO_4^{3-} (DIP) 78

Figure 4.7 Representative raw voltammetric data 81

Figure 5.1 Flow chart of potential processes influencing the biogeochemistry of coral reef ecosystems during spawning events 89

Figure 5.2 In situ instrumentation and weather data collected during coral spawning study 95

Figure 5.3 Data from the acoustic Doppler current-profiler (ADCP) deployed in Gilligan's lagoon 96

Figure 5.4 Isotopic signatures and nutrient ratios of gamete and adult host tissue from 2007 and 2008. 98

Figure 5.5 Lipid concentrations from pre- and post-spawning adult host tissues collected in 2007....99

Figure 5.6 Carbon and nitrogen concentrations and isotopic values of surface and bottom water particulate samples and surface sediments....104

Figure 5.7 Calculated benthic diffusive nutrient fluxes of NH_4^+ and PO_4^{3-} 106

Figure 5.8 Photopigment data from water column particulates. 107

Figure 5.9 Dissolved nutrient concentrations of surface and bottom water samples 109

Figure 6.1 Redox ladder schematic....119

Figure 6.2 Profiles of redox sensitive porewater from sediment cores (adapted from Briggs et al. 2007)....121

Figure 6.3 Schematic of diurnal oscillations in sediment redox conditions....123

Figure 6.4 Aerial photograph of He'eia Fishpond, coastal Kane'ohe Bay, Oahu, Hawai'i....127

Figure 6.5 In situ water quality data from multi-parameter YSI 133

Figure 6.6 Electrochemical profiles from sediment cores collected during diurnal experiments....135

Figure 6.7 Inorganic and organic nutrient profiles from sediment cores collected during diurnal experiments....137

Figure 6.8 Results of the principle factor analysis of water column data....139

Figure 6.9 Electrochemical profiles of O_2, H_2S and Fe^{2+} from sediment cores collected during the diurnal experiments....142

Figure 6.10 Depth of O_2 disappearance, Fe^{2+} appearance, and H_2S appearance during diurnal experiments....147

Figure 6.11 NH_4^+ porewater profile with the modeled parabolic fitting function....149

Figure 6.12 Predicted PO_4^{3-} concentrations plotted versus measured PO_4^{3-} concentrations....152

Figure 6.13 Solid-phase P speciation data generated using the modified SEDEX sequential extraction....153

Figure 6.14 Porewater DOP versus PO_4^{3-} concentrations....155

Figure 7.1 Schematic illustrating OM burial and remineralization in sediments....161

Chapter 1

Introduction and dissertation outline

1.1 Scope of work

The research described in this dissertation examines several aspects of organic matter (OM) remineralization in marine sediments, and addresses fundamental questions that link organic matter supply, sediment redox state, and nutrient cycling, including: (i) How does the quality versus the quantity of OM delivered to coastal marine sediments affect sediment redox state and rates of microbial mineralization of organic matter? (ii) How does the episodic delivery of OM to surface sediments, on a variety of time scales (daily, seasonally), impact sediment nutrient recycling, the magnitude of benthic nutrient efflux, and can it influence water column biological communities? (iii) Over what temporal and spatial scales do microbial respiratory pathways, and the consequent distribution of redox reactive chemical species, oscillate in response to shifts in benthic microbial activity. The research presented here was conducted in and around coastal Kane‘ohe Bay and, as such, reveals some processes that may be unique to coastal systems adjacent to new, volcanogenic islands. However, many of the processes studied in this dissertation are operant in all coastal marine sediments, and insights into processes occurring within the coastal sediments of our study site can be readily extrapolated to other coastal systems.

OM deposited in marine sediments is subjected to degradation and chemical alteration through a complex series of microbial respiratory pathways (e.g., Froelich et al 1979; Burdige 2006). A portion of degraded OM may be recycled into the overlying water as dissolved organic matter or inorganic nutrients, the products of OM remineralization. The residual material is incorporated into sediments, where it can be further degraded during burial. The decomposition and burial of OM in sediments are key processes influencing biogeochemical cycles of nutrients (nitrogen, phosphorus) and carbon in coastal waters on time scales ranging from seasonal fluctuations to long, geologic timescales. Nutrient cycling within coastal and continental margin sediments can account for 10-50% of the yearly primary production in overlying waters (Jorgensen 1983), and most of the organic carbon (94%) preserved in marine sediments is buried in continental margin sediments (Berner 1982; Hedges and Keil 1995). The results of the studies described in this dissertation provide novel insights into the factors controlling OM remineralization and the flux of nutrients at the sediment-water interface, which is

essential to understanding coastal ocean productivity and carbon cycling in the global ocean.

1.2 Dissertation research: Method development

Novel methods were developed as part of this dissertation research, without which it would not have been possible to address key hypotheses articulated in this dissertation. The first portion of this dissertation discusses the analytical method development work. Each new protocol underwent extensive testing using analog phases in order to ensure its applicability to natural marine sediments, as well as to rigorously document its precision and accuracy.

Organic carbon (OC) and total nitrogen (TN) concentration and isotopic composition are crucial parameters for interpreting source, quality, and degree of degradation of OM in marine sediments. Several of the coastal sediment sites examined in this study were enriched in carbonate phases (>50% carbonate minerals), and previously published methods, used to determine organic carbon concentrations and isotopic compositions (recently outlined in Komada et al. 2003), are inapplicable to carbonate-rich sediments. Specifically, the traditional acidification rinse method for preparing sediments results in a loss of labile OC from carbonate-rich sediments. **Chapter 2** describes a method that eliminates the loss of labile OC from carbonate-rich sediments using a combined coulometric-elemental analyzer-mass spectrometer approach for carbon and nitrogen quantification and isotopic analysis. The success of this method for quantifying OC concentration and isotopic composition in carbonate rich sediments permits use of a multi-tracer approach (OC and TN concentration and isotopic composition, and organic molar C:N:P ratios) to examine the source and degradation processes of OM within a range of depositional environments examined in this study.

Marine derived OM is generally more labile than its refractory, terrestrial counterpart (Aller et al. 1996; Cowie and Hedges 1992). In coastal marine environments, suspended particulates and deposited bottom sediments can be dominated by labile, cellular marine-derived OM. The ability to accurately quantify labile organic phosphorus (OP) is essential for quantifying living biomass phosphorus (P) and labile non-living OP, the pools most likely to generate mineralized P to support new cycles of primary

production. The SEDEX sequential extraction technique, used to separately quantify reservoirs of solid phase P in marine sediments, quantifies OP in the final step of the procedure. Therefore, the SEDEX method is not optimal for capturing and quantifying labile OP, which can be solubilized in prior steps and incorrectly quantified as inorganic P. In **Chapter 3** we evaluated the feasibility of inserting a Pre-Extraction step into the 'classical' SEDEX scheme, using the Bligh-Dyer (B-D) solution that solubilizes lipids and thus brings cellular OP into solution, in order to separately quantify labile OP in sediments.

1.3 Dissertation research: Field Studies

In **Chapter 4** variations in source (and therefore lability) of OM was systematically related to rates of OM degradation in coastal marine sediments. In this research, sediment cores collected along a shore-perpendicular transect were incubated and rates of microbial OM remineralization were estimated by examining O_2 consumption, H_2S production, and NH_4^+ accumulation in sediment porewaters. Combining estimates of the efficiency of OM remineralization with an analysis of OM sources, to depositional environments along a land-to-sea gradient, enables us to link the remineralization efficiency directly to OM source (e.g., terrestrial versus marine OM). Thus, providing insight into how OM source can impact preservation of organic carbon in marine sediments.

Depending upon the relative loading of different nutrients to an aquatic system, perturbations in nutrient ratios can shift phytoplankton community composition and influence water column productivity. Emplacement of OM to surface sediments during episodic events can alter sediment redox conditions and consequent nutrient retention/release. The impact of episodic input of labile OM in a coastal ecosystem is evaluated during a *Montipora capitata* coral spawning event in Kane'ohe Bay, Hawai'i. **Chapter 5** explicitly links the biogeochemical characteristics of spawning material to subsequent nutrient recycling pathways of spawn-derived organic material (SDOM). This study presents evidence for a water column phytoplankton bloom event triggered by the episodic input of labile SDOM and the subsequent recycling of nutrients from this OM source.

Finally, in **Chapter 6** we focus on OM remineralization pathways within sediments that influence the spatial distribution of reduction-oxidation (redox) reactive chemical species and dissolved metabolites generated from OM degradation. This research evaluates how the expansion and contraction of the oxygenated surficial sediment layer, driven by diurnal shifts between benthic photosynthesis and respiration, can influence the distribution and porewater accumulation of dissolved inorganic and organic nutrients. The shoaling of the oxic redox transition boundary alters down core distributions of redox reactive chemical species (such as ferrous iron), and influences the depth of the anoxic redox transition boundary (as identified by H_2S accumulation). Two distinct depositional environments were chosen for this research in order to examine the how OM source and physical sediment characteristics can influence these processes.

Chapter 7 concludes with a synthesis of the work presented throughout the dissertation, and examines how each research activity aids in our understanding of OM remineralization in coastal sediments.

Chapter 2

Quantifying organic carbon and nitrogen concentration and isotopic compositions in carbonate-dominated coastal marine sediments

with K. C. Ruttenberg, A. E. Ricardo, E. J. Gier, B. N. Popp

Abstract

Previous methods described for the quantification of organic carbon (OC) and total nitrogen (TN) concentrations in marine sediments using acidification for the removal of inorganic carbon (IC) are inapplicable to carbonate-rich (> 50 % by weight $CaCO_3$) sediments. Traditionally, an acidification rinse method has been applied to remove IC prior to quantification of OC and TN concentrations and isotopic composition. We show that application of this method to carbonate-rich sediments results in loss of labile OC (6.5-75.8 % loss) and nitrogen (0.9-27.9 % loss) during rinsing and, as a consequence, underestimates OC and TN. We describe a method that avoids OC loss using a combined coulometeric-elemental analyzer-mass spectrometer approach for carbon and nitrogen quantification and isotopic analysis. We quantified OC concentrations as the difference between TC and IC using coulometry to directly determine IC, and an elemental analyzer to determine total carbon (TC), thus avoiding problems associated with loss of labile OC during acidification and rinsing of carbonate-rich sediments. Total nitrogen (TN) and nitrogen isotopic values were determined on unacidified bulk sediment using an elemental analyzer-mass spectrometer. Although acidification rinse methods are not suitable for determination of OC and TN concentrations in carbonate-rich sediments, it is the only practical method for the determination of organic carbon $\delta^{13}C$ values. To evaluate whether bulk $\delta^{13}C$ values are compromised by OC loss during an acidification rinse treatment, we used the $\delta^{13}C$-$(C:P)_{org}$ metric for assessing organic matter source.

2.1 Introduction

Organic carbon and nitrogen concentration and isotopic composition are important and well-established parameters for interpreting source, quality, and degree of degradation of organic matter in marine sediments. Previously published methods used to determine organic carbon concentrations and isotopic compositions (recently outlined in Komada et al. 2003) are not appropriate for carbonate-rich (hereafter defined as >50% $CaCO_3$) sediments. In addition, previously published methods do not quantify total nitrogen concentrations and isotope composition in carbonate-dominated sediments. The absence of methods for determining organic carbon and nitrogen concentration and isotopic compositions in carbonate-dominated marine sediments represents a significant gap in our ability to quantify key carbon-cycle parameters in an important class of sedimentary environments. To redress this gap, we evaluated known methods for determining organic carbon and total nitrogen concentrations, as well as nitrogen isotopic values ($\delta^{15}N$) in marine sediments, and find that the most appropriate method for carbonate-rich sediments is a combined coulometeric-elemental analyzer-mass spectrometer approach. Organic carbon isotopic ($\delta^{13}C$) values must be determined on separate, paired splits of carbonate-rich sediment samples, using a suitable acidification rinse method (Komada et al. 2008).

Organic carbon in marine sediments is typically quantified via elemental analyzer after inorganic carbon is removed using a variety of acidification methods. Komada et al. (2008) outline three commonly used methods of acidification: i) the 'vaporous method,' in which samples are exposed to HCl vapor, ii) the 'aqueous method,' in which acid is directly applied to sediments without subsequent rinsing, and iii) the 'rinse method,' in which samples are acidified and then rinsed with Milli-Q ® deionized water (MQ-DI). These methods have significant limitations when applied to carbonate-rich sediments. The vaporous method does not completely remove carbonate minerals when sediments contain >33% carbonate (Hedges and Stern 1984; Komada et al. 2008). The most common method for the removal of inorganic carbon is the aqueous method (Hedges and Stern 1984), wherein samples are acidified, dried and reweighed post-acidification for analysis. However, the formation of hygroscopic salts ($CaCl_2$) occurs when the aqueous method is applied to carbonate-rich samples (see Assessment). Formation of $CaCl_2$

retains moisture and makes it impossible to obtain accurate weights for subsequent quantification of organic carbon and nitrogen contents via elemental analysis. Verardo et al. (1990) omitted drying prior to analysis by applying acid directly to pre-weighed sediments in analysis vessels. This method is impractical for carbonate-rich sediments, however, because the initial (pre-acidification) sample size required is too large to be accommodated by typical vessels used for elemental analysis. While the rinse method avoids the formation of hygroscopic salts and successfully removes inorganic carbon in carbonate-rich sediments, total organic carbon and nitrogen may be underestimated using this treatment due to loss of labile organic carbon (and nitrogen) during rinsing. Our study shows that although the rinse method is not suitable for determination of organic carbon and nitrogen concentrations in carbonate-rich sediments, it is the only practical method for determining organic carbon $\delta^{13}C$ values.

Isotopic data can be used to trace biogeochemical processes in marine environments (e.g., Lehmann et al. 2002), to assess sources and biological transformations of organic matter (e.g., McKee et al. 2002), and are useful in paleoecology studies (e.g., Wooller et al. 2003). $\delta^{15}N$ values are commonly determined on non-acidified sample splits via elemental analyzer coupled to a mass spectrometer. Organic C isotope values in sediments are routinely quantified by analysis of acidified samples. Despite the difficulty in obtaining organic C via acidification methods in carbonate-rich sediments (Komada et al. 2008), we are able to determine useful $\delta^{13}C$ values on acidified samples from our test sample sites using the rinse method of Komada et al. (2008). We discuss the impact of organic carbon loss, unavoidable when employing this rinse method, on resulting $\delta^{13}C$ values (see Assessment). It is worth noting that $\delta^{13}C$ and $\delta^{15}N$ values can not be quantified when employing alternative methods to analyze carbon concentration, such as on the residue of sediments that have been ashed to remove inorganic carbon (Gibbs 1977; Heath et al. 1977), or on evolved CO_2 resulting from oxidization and/or acidification methods (Mills and Quinn 1979).

In this paper we outline a method suitable for determining carbon and nitrogen concentration and nitrogen isotopic composition in carbonate-rich sediments. Because of the high total carbon to total nitrogen ratio (TC:TN) characteristic of carbonate-rich sediments we found it necessary to employ reference material with a high TC:TN ratio in

order to determine nitrogen concentrations. Our study-site transect included a gradient from terrestrial to marine dominated sedimentary organic matter (see Materials and Procedures section), enabling us to employ the coupled $\delta^{13}C$ -$(C:P)_{org}$ metric for identification of organic matter source (Ruttenberg and Goñi 1997a; Ruttenberg and Goñi 1997b) in order to evaluate the consistency of measured isotopic values with anticipated organic matter source.

2.2 Materials and procedures

Sediment collection: Sediment push cores were collected from a shore-perpendicular transect in Kane'ohe Bay, Hawai'i. Four sites with distinctly different sediment sites were sampled, and are hereafter defined as: i) Mangrove (collected under a mangrove canopy); ii) Terrigenous-Dominated (collected from a location proximal to riverine input); iii) Carbonate-Dominated (collected from a location distal to riverine input); and iv) Ocean (collected proximal to a coral reef within the bay). Sample sites were chosen to have distinct sources of organic matter and are characterized by systematically varying concentrations of $CaCO_3$ (see results Table 2.1). Sediment cores were sectioned at 0.25 to 1 cm intervals under an inert (N_2) atmosphere to prevent oxidation artifacts, and subsequently freeze-dried (Krall et al. 2009). From each site a surficial sediment sample and a sample from deeper within the cores (~8.5 cm) was ground with a mortar and pestle, sieved (<125 μm), and stored in a desiccator prior to analysis. The mortar and pestle were cleaned before and after each sample with dichloromethane and methanol to minimize cross-contamination of samples. Samples were analyzed at the Isotope Biogeochemistry Laboratory at the University of Hawai'i, Manoa.

Bulk sediment carbon and nitrogen analyses: Concentrations of inorganic carbon (IC) were quantified on untreated, ground samples using a Model 5011 Carbon Dioxide Coulometer coupled with a Model 5130 Acidification Module (UIC, Inc. Coulometrics) that detects carbon dioxide evolved after the addition of 5 mL 2 N perchloric acid. Optimal sample mass for each site was determined according to sample carbonate content (15-400 mg; Table 2.1) in order to keep CO_2 produced from the acidification of samples

Table 2.1 Method of analysis for carbon and nitrogen concentrations and isotopic compositions and approximate mass used for each analytical procedure. Sample mass for each analysis differs among sample sites due to the variable $CaCO_3$ content at each site.

		Ideal sample mass for analysis			
Method of Analysis	Parameter of Interest	**Mangrove Site (mg)**	**Terrigenous Dominated Site (mg)**	**Carbonate Dominated Site (mg)**	**Ocean Site (mg)**
CN[1]	TC, TN, $\delta^{15}N$	5	40	8	8
CN_{acid}[2]	$\delta^{13}C$, OC_{rinse}[4], TN_{rinse}[4]	5	25	10	10
Coulometer[3]	IC	400	100	20	15
		Calculated $CaCO_3$ (wt%)			
	$CaCO_3$[5]	*1.0*	*6.9*	*76.3*	*91.3*
		Gravimetric Correction Values			
	W_f/W_o[6]	*0.83*	*0.75*	*0.18*	*0.04*

[1] Unacidified samples analyzed with a Carlo Erba NA 2500 elemental analyzer coupled with a mass spectrometer (CN)
[2] Acidified samples analyzed with a Carlo Erba NA 2500 elemental analyzer coupled with a mass spectrometer (CN_{acid})
[3] Unacidified samples analyzed with a Model 5011 Carbon Dioxide Coulometer coupled with a Model 5130 Acidification Module
[4] Values obtained on acidified samples from which acid was removed via successive MQ-H_2O rinses, corrected for mass loss due to IC removed using gravimetric correction given by the following equation (for carbon): wt % OC_{rinse}= (ug carbon detected) / (ug sediment analyzed) * (W_f / W_o)
[5] Determined by converting coulometer IC concentration to wt% $CaCO_3$ assuming all IC is in the form of $CaCO_3$
[6] Initial, dry weights of bulk untreated sediments (W_o) and post acidification dry weights (W_f) allow gravimetric correction to OC_{rinse} and TN_{rinse} to account for mass lost during removal of IC (Hedges and Stern 1984). W_f/W_o values were empirically determined on each sediment interval. Reported values are averaged over surficial and deep intervals for each site and are provided solely as a guide for the application of this method to a different suite of sediment samples.

within the linear range of CO_2 produced from the acidification of pure calcium carbonate reference material, analyzed in parallel with the samples (Table 2.2).

Total carbon (TC) and total nitrogen (TN) concentrations and $\delta^{15}N$ values were quantified on untreated, ground samples using a Carlo Erba NA 2500 elemental analyzer, interfaced via a ConFlo II to a Delta Plus mass spectrometer (Finnigan, Inc), using the integrated signals of masses 44, 45 and 46 (for carbon) and masses 28, 29 and 30 (for nitrogen). Samples were weighed into 5 x 9 mm tin capsules (Costech Analytical ®), pre-cleaned by soaking in acetone. Sediment organic carbon concentrations (OC_{diff}) were determined as the difference between TC (measured by mass spectrometry) and IC (measured using coulometry).

Carbon and nitrogen isotopic values are reported using conventional δ-notation with respect to VPDB and atmospheric N_2, respectively. Sample weights were adjusted (5-40 mg; Table 2.1) so that abundances of C and N fell within the range of glycine and acetanilide laboratory reference materials. We found it difficult to obtain accurate

Table 2.2 Carbon and nitrogen contents and isotopic compositions of laboratory reference materials utilized for elemental (CN) analyzer (glycine, acetanilide, and peach leaves) and coulometer ($CaCO_3$) analyses.

	Glycine[1]	Acetanilide[2]	Peach Leaves[3]	$CaCO_3$[4]
Carbon (wt %)	32.0	71.0	45.3	12.0
$\delta^{13}C$ (‰)	-35.8	-30.9	-	-
Nitrogen (wt %)	18.7	10.4	2.8	-
$\delta^{15}N$ (‰)	11.3	-12.1	-	-
Carbon Range (ug C)[5]	20-150	100-1200	-	250-4800
Nitrogen Range (ug N)[5]	15-200	-	<1-15	-

[1]Glycine 99.5% Assay CAS #56-40-6
99% [2]Acetanilide Assay CAS #103-84-4
[3]NIST SRM 1547
[4] Reagent grade $CaCO_3$ CAS #471-34-1
[5]Suggested abundance range of reference material needed for instrument calibration for the samples analyzed in this study

weights of glycine and acetanilide needed for instrument calibration at low TN even using a 6-place balance (UMX2, Mettler Toledo). To extend the instrument calibration to low TN concentrations when analyzing carbonate-rich samples with high TC:TN, we used a National Institute of Science and Technology (NIST) certified reference material (peach leaves, NIST SRM1547; Table 2.2). The peach leaves reference material has a relatively high TC:TN, allowing u to weigh out measurable quantities of standard, with low nitrogen content, thus extending our standard curve to lower values.

Acidified samples for carbon isotopic analyses of organic matter were prepared using the rinse-acidification method modified after Komada et al. (2008). This analysis also provided organic carbon (OC_{rinse}) and nitrogen (TN_{rinse}) concentrations, which were utilized to assess quantity of OC and TN lost during acidification and rinsing. Dry, ground sediment samples from each location were weighed into pre-weighed centrifuge tubes (W_o). IC was removed by slowly adding 3 N hydrochloric acid, until no effervescence was detected. The required quantity of acid varied depending upon $CaCO_3$ concentration but was roughly between 10-50 ml for all samples (sample mass range: 300-2500 mg; Table 2.1). The acid and three consecutive MQ-H_2O rinses were removed via centrifugation and decanting. The acid-treated sediments were dried at 60ºC, re-weighed to determine final weight (W_f), and stored in a desiccator until analysis. Carbonate-free samples were weighed (5-25 mg; Table 2.1) and analyzed isotopically as above. Values were corrected for mass loss during acidification and IC removal by applying a gravimetric correction (Hedges and Stern 1984) using the following equation (given for carbon):

$$\text{wt\% } OC_{rinse} = (\mu g \text{ carbon detected}) / (\mu g \text{ sediment analyzed}) * (W_f / W_o) \quad (2.1)$$

Bulk sediment phosphorus analysis: Inorganic sedimentary phosphorus (IP) was determined utilizing the acid hydrolysis method of (Aspila et al. 1976) and total sedimentary phosphorus (TP) was determined using the high-temperature ashing/hydrolsis method of (Monaghan and Ruttenberg 1999). Organic phosphorus (OP) was determined as the difference between TP and IP.

End member analysis: The following samples were collected to characterize end member source material: (i) *Rhizophora mangle* propagules, seeds, leaves, and root material from a coastal mangrove forest in Kane'ohe Bay; (ii) *Acanthophora* sp. and *Gracilaria* sp., macroalgae found in Hawaiian coastal waters; and (iii) plankton collected from within Kane'ohe Bay using a 100 μm tow net. End member samples were freeze-dried and homogenized prior to analysis for organic carbon and total nitrogen concentrations and isotopic values, using the aqueous method described by Komada et al. (2008) to avoid soluble OC loss during rinsing. Inorganic and total phosphorus were analyzed using the previously discussed methods.

Error estimation: Errors were estimated using the following methods: (i) propagation of analytical errors, (ii) Monte Carlo simulation of analytical error, and (iii) calculation of precision based on duplicate sample analysis. Propagation of analytical error assumed uniform distribution of instrument standard deviations and resulted in the largest propagated uncertainties. In the Monte Carlo simulation we assumed normal distribution of instrument uncertainty, such that the mean value represented the most probable value, and instrument uncertainty was within the 95% confidence intervals of the distribution function. The Monte Carlo simulation was run over 100,000 iterations and yielded slightly lower uncertainties (Anderson 1976). Each sample was analyzed in duplicate and the uncertainty was estimated as the difference between the duplicate results. Calculation of precision over duplicate analysis, which implicitly includes instrument analytical uncertainty, produced the lowest estimate of analytical error. We chose to report here uncertainty based on Monte Carlo simulations, since these provided an intermediate value of uncertainty (Table 2.3).

Table 2.3: Carbon and nitrogen concentrations of sediment samples collected at two discrete depth intervals (near-surface and deep) at each site. All values reported are the average over duplicates; errors determined via Monte Carlo simulation are shown in parenthesis.

Site	Depth (cm)	TC (wt %)	IC (wt %)	OC_{diff}[1] (wt %)	OC_{rinse}[2] (wt %)	TN (wt %)	TN_{rinse}[2] (wt %)	% loss[3] OC	% loss[3] TN
Mangrove	1.3	7.89 (0.20)	0.12 (0.00)	7.77 (0.20)	7.12 (0.18)	0.494 (0.0012)	0.489 (0.012)	8.2	0.9
Mangrove	8.6	5.60 (0.14)	0.10 (0.00)	5.50 (0.14)	5.16 (0.13)	0.356 (0.009)	0.342 (0.009)	6.5	4.5
Terrestrial Dominated	1.3	1.78 (0.05)	0.70 (0.00)	1.08 (0.05)	0.81 (0.02)	0.054 (0.001)	0.039 (0.001)	25.2	27.7
Terrestrial Dominated	8.3	2.10 (0.05)	0.67 (0.01)	1.43 (0.05)	1.21 (0.03)	0.065 (0.002)	0.050 (0.001)	15.2	27.8
Carbonate Dominated	1.3	10.43 (0.26)	9.52 (0.10)	1.00 (0.28)	0.22 (0.01)	0.022 (0.001)	0.019 (0.000)	75.8	10.6
Carbonate Dominated	8.4	9.70 (0.24)	9.01 (0.09)	0.70 (0.26)	0.19 (0.00)	0.020 (0.000)	0.016 (0.000)	72.8	19.7
Ocean	2.1	11.29 (0.28)	10.97 (0.11)	0.33 (0.30)[4]	0.10 (0.00)	0.015 (0.000)	0.013 (0.000)	68.4	12.5
Ocean	8.5	11.17 (0.28)	10.95 (0.11)	0.23 (0.30)[4]	0.17 (0.00)	0.014 (0.000)	0.023 (0.001)	18.7	-

[1]Calculated as: $OC_{diff} = TC - IC$

[2]Organic carbon $(OC)_{rinse}$ and total nitrogen $(TN)_{rinse}$ values were obtained through analysis of acidified samples. Acid was removed via three successive MQ-H_2O rinses of sediments. Gravimetric correction for mass loss due to IC removal was calculated using equation 1.

[3]Values reflect estimates of OC and TN loss during acidification and subsequent rinses during IC removal prior to elemental analysis (see text for more complete discussion and equations).

[4]Error values obtained through analysis of duplicate samples yielded smaller uncertainties, indicating higher precision than expected based on reported Monte Carlo error propagation (see Comments and Recommendations)

2.3 Assessment

Carbon and nitrogen concentrations: Traditionally IC is calculated as the difference between TC and OC, measured using an elemental analyzer on untreated and acidified samples, respectively. We chose not to use acidified splits to determine OC concentrations because we were leery of OC loss during acidification and subsequent rinses. Instead we used coulometry to directly determine IC, and then used TC and IC to calculate OC by difference (OC_{diff}). As is the case for all difference methods, it is essential to obtain precise values for measured parameters (TC and IC in this case) in order to minimize error, and to propagate those errors when calculating the derived parameter and its uncertainty.

Figure 2.1 A typical nitrogen quantification curve for the Carlo Erba NA 2500 elemental (CN) analyzer. The linear range for mass of nitrogen obtained by integrating the peak area for masses 28, 29 and 30 for the glycine laboratory reference compound (15-100 μg N) is extended to lower values (1-15 μg N) using the NIST SRM1547 Peach Leaves certified reference material.

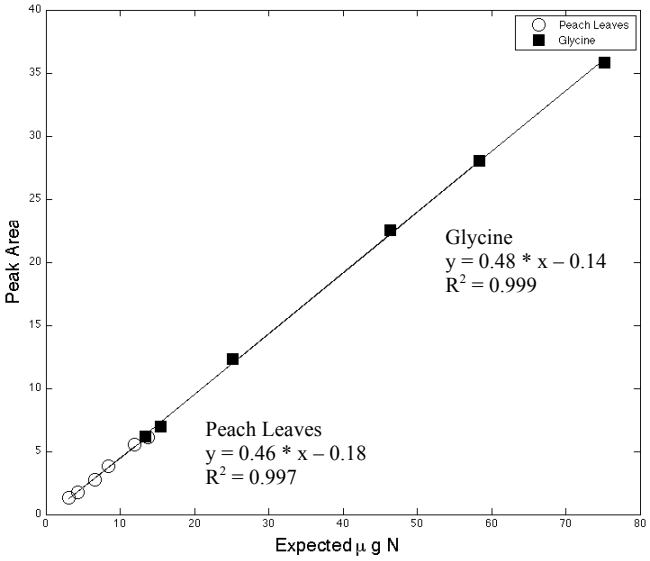

Quantification of total nitrogen proved challenging for carbonate-rich sediments because they typically have elevated TC:TN ratios, owing to the high IC content (Table 2.3). In order to achieve a sufficient instrument response necessary to determine N abundance and isotopic composition of the carbonate-dominated ocean sediments analyzed, large sample masses (35-45 mg) were required when using instrument response curves based only on the glycine and acetanilide reference materials. These large sample masses caused unacceptable increases in baseline between samples and inconsistent reproducibility. To address this problem, we extended the lower range of N quantification using a reference material with a high TC:TN ratio (NIST SRM1547, peach leaves; Figure 2.1) relative to the other reference materials. The low concentration of N in peach leaves, relative to C, allowed us to accurately weigh quantities of

SRM1547 needed to generate a reliable quantification curve, which allowed us to determine N concentrations of carbonate-rich sediments using a reasonable sample mass (~8 mg; Table 2.1). Although TN abundance could be determined reliably with this method on samples with less than ~15 μg N, the uncertainty in the measured $\delta^{15}N$ values of laboratory reference materials within this TN range became unacceptably large (>0.5‰).

Although samples prepared using the rinse method were used principally to allow measurement of $\delta^{13}C$ values, the OC_{rinse} and TN_{rinse} results allowed us to also evaluate the percent loss of carbon and nitrogen due to the post-acidification rinses (Table 2.3). After gravimetric correction (Equation 2.1), the % loss of OC was calculated using the following equation (given for carbon):

$$\% \text{ loss OC} = (OC_{diff} - OC_{rinse}) / OC_{diff} * 100 \quad (2.2)$$

Loss of organic carbon ranged from 6.5% in deep Mangrove sediment up to 75.8% of total OC in shallow carbonate sediments. Percent loss of carbon was greater in surficial sediment intervals (Table 2.3), which we attribute to the greater solubility of labile organic matter present within young surficial sediments relative to the more refractory organic matter found in more deeply buried sediments (Hedges and Keil 1995). The rinse method is known to cause loss of a fraction of organic matter (Froelich 1980), thus OC determined on acidified samples is underestimated (Table 2.3). The alternative method proposed here, in which IC determined directly via coulometry is subtracted from TC to derive OC, does not suffer from OC loss during sample preparation, and is therefore a more accurate method for the quantification of OC.

Carbon and nitrogen isotopic compositions: Although OC and TN losses during the rinse method are unavoidable, IC must be quantitatively removed from sediments via acidification prior to determination of $\delta^{13}C$ values of organic carbon. We found no practical alternative to the rinse method for the determination of $\delta^{13}C$ values of carbonate-rich sediments. Initial trials utilizing the vaporous method (Komada et al. 2008) on carbonate-rich samples did not completely remove all carbonate material. Trials of the aqueous method without MQ-H_2O rinses (Hedges and Stern 1984) required a large

Table 2.4 $\delta^{13}C$ and $\delta^{15}N$ values for sediment samples collected at two discrete depths from each site. All values reported are the average over duplicates; maximum instrumental error is ± 0.2‰. End member isotopic values are best estimates for local (Hawai'i) source organic material; elemental $(C:P)_{org}$ are also reported for end members.

Site	Depth (cm)	$\delta^{13}C$ (‰)	$\delta^{15}N$ (‰)
Mangrove	1.3	-25.7	1.4
Mangrove	8.6	-24.8	2.1
Terrestrial Dominated	1.3	-22.1	1.8
Terrestrial Dominated	8.3	-24.3	1.5
Carbonate Dominated	1.3	-15.3	1.8
Carbonate Dominated	8.4	-16.4	3.7
Ocean	2.1	-16.4	3.5
Ocean	8.5	-17.2	3.5

End member	$C:P_{org}$	$\delta^{13}C$ (‰)	$\delta^{15}N$ (‰)
Mangrove end member[1]	1321:1 to 782:1	-27.0 to -28.8	-0.3 to 2.6
Macroalgae end member[2]	5809:1 to 1572:1	-17.7 to -16.6	0.0 to 3.8
Phytoplankton end member[3]	268:1	-19.0 ± 0.1	6.8 ± 0.3

[1]Values from *Rhizophora mangle* in He'eia Fishpond.

[2]Values from macroalgae (*Acanthophora* sp. and *Gracilaria* sp.) found within He'eia Fishpond. High ratios are due to structural carbon found in fleshy marine algae.

[3]Values from a plankton tow conducted in Kane'ohe Bay. Phytoplankton $(C:P)_{org}$ ratios are markedly higher than the Redfield ratio for marine phytoplankton. We suspect that this elevated value is a consequence of inclusion of small fragments of high $(C:P)_{org}$ macroalgae and terrestrial vegetation in the net tow material that persisted despite our attempts to remove fragments of non-phytoplankton organic matter from this sample.

quantity of acid (see Method) to completely remove all carbonate material. This resulted in the formation of a hard, dry coating of hygroscopic salt ($CaCl_2$), which trapped moisture such that the bulk of the acidified sediments never dried, even at temperatures exceeding 160ºC for several days. Thus, rinse-acidification seems the only viable method for the removal of inorganic carbon in carbonate-rich samples, despite the fact that some organic carbon is lost due to solubilization and subsequent rinsing (Table 2.3).

Partial loss of organic carbon during rinsing after acidification could potentially alter $\delta^{13}C$ values. If the organic matter lost during acidification has a carbon isotopic composition distinct from the bulk organic matter within the sediments, the $\delta^{13}C$ values obtained after rinse-acidification may not be an accurate representation of bulk sediment $\delta^{13}C$ values. To investigate the extent to which $\delta^{13}C$ values obtained using the rinse method might have been impacted by organic carbon loss, we employed the coupled $\delta^{13}C$-$(C:P)_{org}$ metric (Ruttenberg and Goñi 1997a; Ruttenberg and Goñi 1997b) to evaluate whether sample

$\delta^{13}C$ values were consistent with end member source materials in the environments studied. Since our stations were arrayed along a transect that spanned a gradient from terrestrial- to marine-dominated organic matter, we can contrast sedimentary $\delta^{13}C$ values to the isotopic and elemental composition of end-member terrestrial and marine organic matter, and assess the extent of deviation from expected trends.

Marine phytoplankton have a mean molar organic $(C:P)_{org}$ of 106:1 (Redfield et al. 1963) in contrast to terrestrial, vascular plants, which have characteristic $(C:P)_{org}$ up to or exceeding 800 (Likens et al. 1981). Isotopic compositions of local marine phytoplankton and mangrove are reported (Table 2.4) for comparison against our sediment samples. A plot of $(C:P)_{org}$ versus $\delta^{13}C$ values of organic matter produces a hyperbolic trend characteristic of the mixing line between two-end member materials (marine phytoplankton vs. vascular plant) on a ratio-to-ratio plot, as described by Ruttenberg and Goñi (1997a; 1997b); Figure 2.2). This trend illustrates that the sediments along our shore-perpendicular transect reflect a smoothly varying progression between the two end-members. Thus, inadvertent removal of organic carbon during the rinse-acidification method did not measurably affect the characteristic isotopic signatures of the bulk sediments analyzed. It is preferable to determine total nitrogen concentration and $\delta^{15}N$ values on bulk, untreated sediment samples to avoid the complication of nitrogen loss during the acidification rinse method. We determined TN and $\delta^{15}N$ values on bulk sediments from our two sites that contained <50% $CaCO_3$, the mangrove and terrigenous dominated sites. Due to the high TC:TN ratios of the two sites with >50% $CaCO_3$, the TN concentrations of optimal sample mass fell below the threshold of accurate nitrogen isotopic analyses of reference materials (see previous discussion). Therefore, $\delta^{15}N$ values of carbonate-rich sediments, such as the carbonate-dominated and ocean site samples in this study were obtained from samples subjected to the acidification rinse method. Because the acidification rinse method results in loss of total nitrogen (Table 2.3), one must assume that loss of material does not result in a shift in the $\delta^{15}N$ value of bulk sediment. The $\delta^{13}C$-$(C:P)_{org}$ analysis discussed earlier (Figure 2.2) suggested that artifacts resulting from the acidification rinse method did not significantly alter sediment $\delta^{13}C$ values, so we make a similar assumption for $\delta^{15}N$ values. It was not possible to employ a similar analysis (e.g., $\delta^{15}N$-$(C:N)_{org}$) to evaluate the integrity of the nitrogen isotopic

compositions of samples (data not shown). TN concentrations and $\delta^{15}N$ values are significantly altered during early diagenesis (e.g., Freudenthal et al. 2001), and thus cannot be used to asses organic matter sources. The TN and $\delta^{15}N$ values are however useful to understand biogeochemical transformation in sediments (e.g., Lehmann et al. 2002).

2.4 Discussion

Previous methods described for the quantification of organic carbon and total nitrogen concentrations and isotopic composition are inapplicable to carbonate-rich (> 50% by weight $CaCO_3$) sediments. Our method overcomes the limitation of these published methods by employing a combined coulometric-elemental analyzer-mass spectrometer approach for carbon and nitrogen quantification and isotopic analysis. Using coulometry to directly determine IC, we quantified organic carbon concentrations as the difference between TC and IC, thus avoiding problems associated with loss of labile OC during acidification of carbonate-rich sediments. Use of a reference material with a high TC:TN ratio (NIST Peach Leaves) allowed quantification of TN in high TC:TN carbonate-rich samples using a workable sample mass. Because removal of inorganic carbon from sediments is required prior to analysis for organic carbon isotopic composition, it was necessary to use the acidification rinse method to determine organic

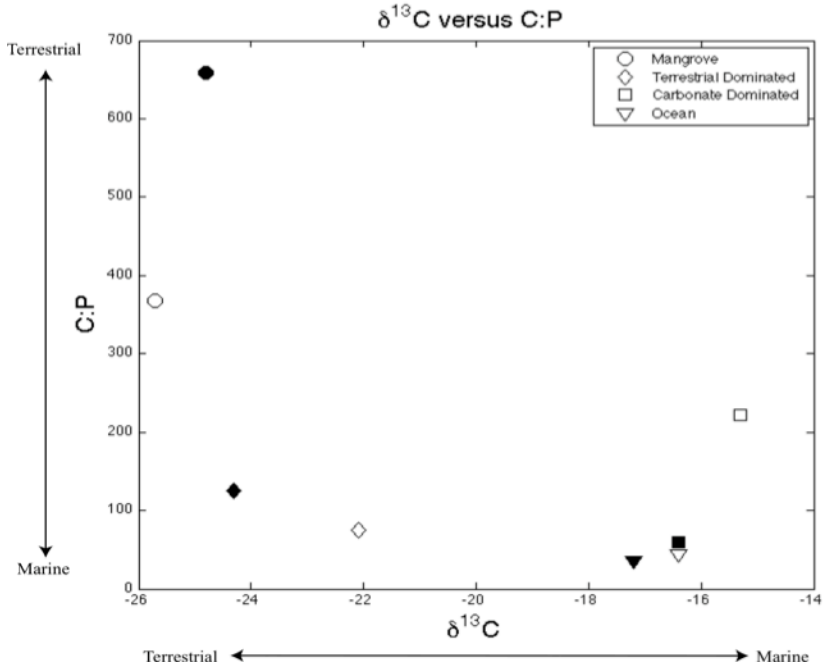

Figure 2.2 Organic carbon $\delta^{13}C$ values plotted against molar $(C:P)_{org}$ ratios permit evaluation of the source of organic matter to sediments. The upper left corner is representative of terrestrial material, characterized by high $(C:P)_{org}$ and low $\delta^{13}C$ values, whereas the lower right corner is indicative of marine material, characterized by low $(C:P)_{org}$ and higher $\delta^{13}C$ values (see Table 4). Open symbols represent surficial sediments at each site; filled symbols are taken from deeper within the sediment core (see Table 2.3

carbon $\delta^{13}C$ values. Application of the $\delta^{13}C$-$(C:P)_{org}$ metric for assessing source of organic matter suggests that the source signal of bulk $\delta^{13}C$ values was not compromised by OC loss during the acidification rinse method.

2.5 Comments and Recommendations

The ideal samples masses and W_f/W_o data presented in this paper were determined using trial and error (Table 2.1), and are specific to our sample sites. These values are provided solely as a guide for the application of this method to new sediment samples. Optimal values may vary based upon sample composition and organic matter lability as well as with the instrumentation used. Therefore, any analyst employing this method should independently verify ideal sample masses for optimal results.

Although it is not possible to independently quantify the effects of organic carbon loss on $\delta^{13}C$ values of sedimentary organic matter during the acidification rinse method, results of the $\delta^{13}C$-$(C:P)_{org}$ analysis (Figure 2.2) suggest that any losses did not obscure organic matter source information. However, it would be prudent to measure the percent loss of OC, and if possible its affect on bulk sediment $\delta^{13}C$ values, when applying the acidification rinse method to other environments. Such an assessment is likely to be particularly crucial for sediments containing labile organic matter, as a larger fraction of labile OC will likely be lost.

Recognizing the importance of obtaining accurate and robust estimates of analytical uncertainty of measurements, we compared the uncertainties obtained by 3 independent approaches (see Method section). In several instances the Monte Carlo approach yielded large uncertainties that may be unrealistic. The uncertainty obtained through analysis of duplicate samples typically yielded smaller uncertainties, indicating higher precision than expected based on Monte Carlo error propagation (data not shown). For example, OC_{diff} of the two ocean samples are reported as 0.33 ± 0.30 and 0.22 ± 0.30 wt% using the Monte Carlo simulation (Table 2.3); however, precision calculated from duplicate analysis of the same ocean samples yielded reproducibility of 0.33 ± 0.06 and 0.22 ± 0.00 wt%, respectively. Monte Carlo errors are reported to provide a conservative estimate of uncertainty. However, we suggest that error calculated over replicate analyses is equally valid, and may be a more realistic estimate of uncertainties.

Acknowledgements

Miguel Goñi supplied important suggestions that guided initial stages of method development, which we gratefully acknowledge. We thank Craig Glenn for access to his coulometer. This research was supported by a grant/cooperative agreement from the National Oceanic and Atmospheric Administration; project R/EL-42, which is sponsored by the University of Hawai‘i Sea Grant College Program, SOEST, under Institutional Grant NA05OAR4171048 from NOAA Office of Sea Grant, Department of Commerce. The views expressed herein are those of the authors and do not necessarily reflect the views of NOAA or any of its sub-agencies. UNIHI-SEAGRANT-xxxx. This is SOEST contribution #x

Chapter 3

Evaluation of Novel SEDEX Extraction Steps for Labile Organic Phosphorus and $CaCO_3$-bound Phosphorus in Aquatic Sediments

with K. C. Ruttenberg

Abstract

This study evaluates the merits of two proposed modifications to the 'classical' SEDEX scheme for sequential extraction of different forms of P from sediments, targeting labile organic phosphorus (L-OP) and calcium carbonate-bound phosphorus ($CaCO_3$-P). The selectivity and efficiency of a Bligh Dyer-type lipid extraction technique was analyzed for separately quantifying labile organic phosphorus in aquatic suspended particulate matter and bottom sediments. Monospecific phytoplankton cultures were used as 'analogues' for labile particulate organic matter. Our objective was to insert a step to precede the full SEDEX method that will remove the labile portion of the OP pool, prior to subjecting samples to the harsher extractants that make up the balance of the SEDEX scheme. Although the SEDEX method includes a step for quantifying OP, it is not optimal for capturing and quantifying labile OP because in the current scheme OP is quantified in the final step. Thus, labile OP can be solubilized in prior steps and incorrectly quantified as inorganic P. The ability to accurately quantify labile OP is essential for quantifying living biomass P and labile non-living OP, the pools most likely to generate mineralized P to support new cycles of primary production. This modification could be particularly important for aquatic suspended particulates or newly deposited bottom sediments, which may be dominated by labile, cellular material. The insertion of a tri-ammonium citrate extraction step prior to Step IIIA of the SEDEX method is evaluated for its ability to efficiently and selectively extract $CaCO_3$-P prior to extraction of other reactive Ca-P phases (authigenic carbonate fluorapatite and biogenic hydroxyapatite), which are targeted in SEDEX-Step III.

3.1 Introduction.

Selective, sequential extraction methods are widely used for separately quantifying different forms of phosphorus (P) in sediments and soils (e.g., Krall et al. 2009, Lukkarri et al. 2009, Monbet et al. 2009, Slomp et al. 2006). One method that has been particularly widely used in the study of marine sediments is the SEDEX method (Ruttenberg 1992; Ruttenberg et al. 2009), which separately quantifies five P reservoirs, in the following order: (Step I) exchangeable or loosely sorbed P, (Step II) ferric iron (Fe) bound P, (Step III) authigenic and biogenic apatite plus $CaCO_3$-bound P, (Step IV) detrital apatite and other inorganic P, and (Step V) organic P. As is the case with all selective extraction methods, the SEDEX method is operationally defined, and was exhaustively calibrated using analogue phases to confirm the specificity for the phase targeted for extraction in each step of the SEDEX scheme (Ruttenberg 1992).

Despite its careful standardization, the operationally defined nature of SEDEX leads to inherent uncertainties in the determination of sediment-P distribution and, where possible, it is valuable to refine the specificity of the method. Two SEDEX-defined P reservoirs have received such additional attention since the method was first proposed in 1992: The combined reactive Ca-P reservoir targeted in Step III, and the organic P (OP) reservoir targeted in Step V. For example, Shenau et al. (2000) introduced an additional step into the SEDEX scheme that permits the separate quantification of fish bones (biogenic, hydroxyapatite: HAP), which are otherwise extracted in tandem with authigenic apatite (CFA) plus $CaCO_3$-bound P in Step III. This step may be particularly important for coastal upwelling regions, where fish production can lead to large inputs of HAP to underlying sediments. Vink et al. (1997) proposed adding a step to enable extraction of OP earlier in the scheme, to avoid its premature extraction in Steps I-IV. Neither of these proposed modifications to the SEDEX method have been widely adopted, likely due to the work-intensive nature of each, as both involve multiple extractions. In this paper, we present results of experiments conducted to test two novel SEDEX steps to separately quantify these same two P-reservoirs: reactive Ca-P and labile-OP.

It has been previously recognized that because extraction of OP occurs as the final step of SEDEX (Step V), the potential exists for premature extraction of *labile* organic

Figure 3.1 SPExMan-SEDEX scheme for different forms of P in marine sediments (Ruttenberg et al. 2009) illustrating insertion of Pre-Extraction step for L OP recovery prior to Step I, and insertion of the TAC extraction for separate quantification of $CaCO_3$-P prior to Step IIIA

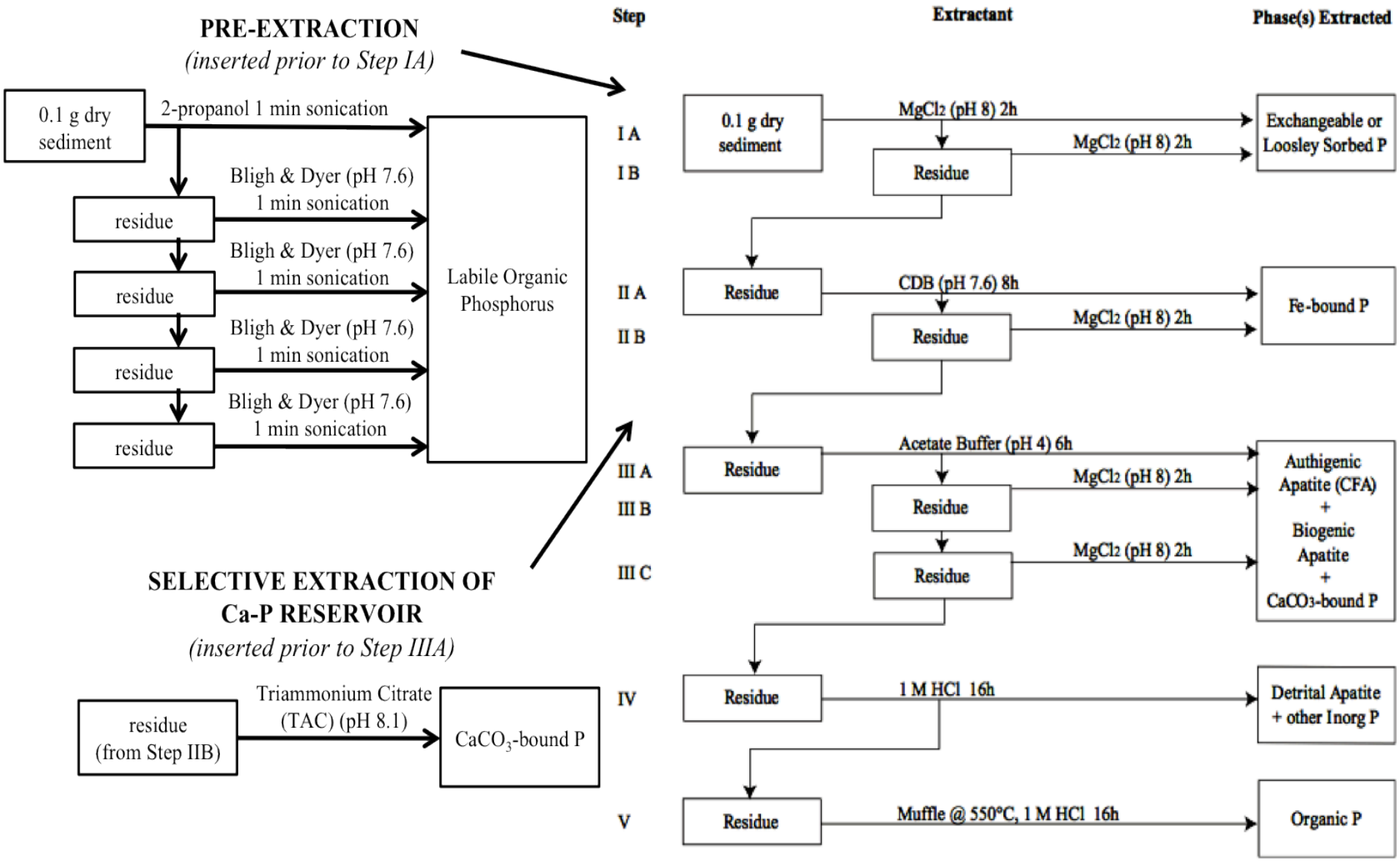

P (L-OP) in prior SEDEX steps. If solubilized and hydrolyzed, this dissolved organic P (DOP) would be erroneously included in one of the inorganic P (IP) reservoirs. If solubilized but not hydrolyzed, this prematurely extracted DOP would be unaccounted for in the final SEDEX P-distribution (Ruttenberg 1992; Vink et al. 1997). In its initial formulation the SEDEX method was developed for application to marine sediments, and Ruttenberg (1992) argued that the likelihood of significant OP loss in Steps I-IV was minimal because seabed sediments are more likely to be dominated by older, more degraded and refractory organic matter. In fact, solubilization of a portion of OP from in Steps I-IV was documented in test sediments (Ruttenberg 1992), but this quantity was fairly small (<10% of total-P (TP)) and, because it was solubilized without being hydrolyzed, did not contribute OP to the IP reservoirs solubilized in Step I-IV.

One cannot ignore the risk of premature extraction of L-OP, however, if the SEDEX method is applied to aquatic suspended sediments, which may be comprised in large part by cellular (planktonic) P, or to surface sediments that are the recipient of L-OP as the result of high overlying water primary productivity. This paper summarizes the evaluation of a Pre-Extraction step, inserted prior to Step I of the SEDEX scheme (Figure 3.1), designed to remove the labile portion of the OP pool prior to subjecting samples to the harsher extractants that make up the balance of the SEDEX scheme. In addition, we present results of experiments designed to evaluate the possibility of separately quantifying $CaCO_3$-bound P (hereafter $CaCO_3$-P), as distinct from CFA and HAP (Figure 3.1).

3.2 Materials and Methods

General strategy: Adopting the rationale of standardization experiments designed to evaluate the original SEDEX method (Ruttenberg 1992), three types of experiments were preformed: (i) efficiency experiments, designed to confirm the extent to which complete recovery of target phases (either L-OP or $CaCO_3$-P) was achieved, (ii) specificity experiments to examine the extent of dissolution of solid P reservoirs other than target phases in the proposed new extraction steps, and (iii) matrix effect experiments designed to examine the potential re-adsorption of P solubilized from target

phases onto surfaces of other (non-target, or matrix) phases that remain in tact during the extraction step.

Because of the operationally defined nature of SEDEX, it is critical to standardize the proposed extraction steps with materials that closely approximate naturally occurring materials (Table 3.1). Pure cultures of three algal taxa, grown under nutrient replete conditions, were used as analogues for L-OP. Cultured algae were washed with 1M ammonium formate solution prior to freeze drying to remove any non-cellular P and residual salts in the culture media. In addition to pure cultures, a mixed plankton assemblage recovered in a net tow from Long Island Sound (Ruttenberg 1992) was used as an analogue for field-collected, suspended particulate L-OP. Reagent grade $CaCO_3$ was used as an analogue for naturally occurring carbonate phases. Discrete mineral phases used for efficiency, specificity and matrix effect experiments are similar to those

Table 3.1 Analog phases used for Pre-Extraction experiments. (*) For specificity experiments pure minerals were pre-sorbed with P by shaking pure mineral phases in a saturated solution of inorganic P (10 mM P). Uncertainties are reported as standard error based on replicate analyses

Analog Phase	Total P (pre-sorption) µmol P/ g	Total P (sorbed to mineral) µmol P/ g	Source
Bulk Plankton	90.5 ± 0.7	N/A	Collected via net tow in Long Island Sound (Ruttenberg 1992)
Green algae	284 ± 3	N/A	*Tetraselmis chuii*; cultured at WHOI
Diatom	337 ± 13	N/A	*Thalassiosira pseudonana*; cultured at WHOI
Dinoflagellates	232 ± 10	N/A	*Heterocapsa* and *Lingulodinium polyedrum*; cultured at WHOI
Ferrihydrite*	N/A	279 ± 9	Synthesized according to Schewtmann and Cornell (1991)
Goethite*	N/A	54.4 ± 1.7	Synthesized according to Schewtmann and Cornell (1991)
Calcite*	N/A	0.34 ± 0.02	Baker analyzed pure $CaCO_3$
Aragonite*	N/A	1.25 ± 0.04	Collected in Kaneohe bay, Hawai'i; confirmed via XRD analysis
Smectite*	N/A	10.1 ± 0.8	Cutter Cermaics (Ruttenberg 1992)
Kaolinite*	N/A	17.7 ± 0.3	Fisher Scientifict kaolin, acid washed, Cat. No. K5-500 lot No. 761094 (Ruttenberg 1992)
CFA nodule	N/A	4106 ± 82	(Ruttenberg 1992)

used by Ruttenberg (1992), and for the purpose of efficiency and specificity experiments, were loaded with surface-sorbed phosphate by pre-equilibration in a 10 mM phosphate solution, as in Ruttenberg (1992).

Extractants and extraction approach: We have chosen to use the Bligh-Dyer (B-D) extractant, a well-proven medium for extracting lipids from particulate organic material (Bligh and Dyer 1959), to selectively solubilize L-OP from aquatic particulate material in the Pre-Extraction step. The B-D extractant is a single-phase water:methanol:chloroform (0.8:2:1) solution that efficiently extracts polar lipids. For this study, two modifications to the Bligh and Dyer method were adopted (Laarkamp 2000): (i) the sediment-solvent mixture was sonicated with a Tekmar® sonic disrupter probe to ensure complete recovery of intracellular OP, and (ii) a single 2-propanol extraction was conducted prior to B-D solvent extraction to deactivate lipases, preventing degradation of phospholipids during extraction. A 0.5 M solution of tri-ammonium citrate (pH 8.1), so called 'Silverman's Solution', was chosen for the selective dissolution of $CaCO_3$-associate P from carbonate fluorapatite because carbonate-fluorapatite is relatively insoluble (solubility = 0.012 g / 100 ml solution), as compared to calcium carbonate (solubility = 0.660 g / 100 ml solution) in this solution (Silverman et al. 1952).

The SPExMan extraction manifold (Ruttenberg et al. 2009) was used for all experiments in this study. Manifold reaction vessels, filter holders, stopcocks and caps are Teflon, which is essential in order to withstand exposure to the B-D solvent mixture, which would degrade other commonly-used plastics such as polycarbonate, polypropylene, polyethylene, etc. Reaction vessel diameter (20 mm) is large enough to accommodate the Tekmar sonic disrupter probe (10 mm), allowing samples to be sonicated within the reaction vessels.

GH polypropylene (GHP) filters (0.2 µm; Pall Life Sciences©), a hydrophilic universal membrane filter, were the filter of choice as they were expected to provide maximum chemical compatibility with both aqueous solutions and aggressive solvents; the polycarbonate (PC) filters recommended for the SPExMan-SEDEX protocol (Ruttenberg et al. 2009) are incompatible with the Pre-Extraction B-D solvent mixture. To verify the filter suitability, we examined the effects of physical sonication, as well as solvent and reagent exposure, on the integrity of the GHP filter. GHP filters were brought

through the Pre-Extraction step followed by the full SEDEX method (Figure 3.1), and also taken through the Pre-Extraction sonication and SEDEX steps replacing solutions with MQ-DI, as a control for effects of physical manipulation in the absence of solvent exposure. Filters were thoroughly rinsed with MQ-DI at the end of each experiment, dried at room temperature and cut in half. Half of the filter was prepared for Scanning Electron Microscope (SEM) viewing to visually ascertain filter integrity, and the other half was combusted according to Step V of SEDEX.

Phosphorus analysis of supernatants: Total Dissolved P (TDP) was quantified in Pre-Extraction solvents (both 2-proponal and the B-D solvent mix) using a modified high-temperature ashing method (Laarkamp 2000). Extractants (total volume: 13 mL) were adjusted to pH 1 with trace metal clean concentrated hydrochloric acid (HCl; 100 µL) and spiked with 50% (w/v) $Mg(NO_3)_2$ (560 µL). Samples were dried at 60˚C for several days. When samples appeared dry, the oven temperature was increased to 120˚C for 2 hours to ensure complete dryness, which is critical to prevent spattering during the muffling step. Each vial was tightly covered with muffled Al foil squares and combusted for 2 hours in a muffle furnace at 550˚C. Once cooled, 1M HCl (6.5 mL) was added to each vial, and vials were shaken on a horizontal shaker table at 300 rpm for 16 hours. After the 16-hour extraction was completed, 12 N NaOH was added (200 µL) to bring the solution to a final pH of 1. Samples were analyzed for TDP on a BioTek Synergy HT Multi-Mode microplate Reader using the molybdate-blue colorimetric method (Grasshoff, 1972). Because of citrate interference with colorimetric protocols for phosphorus (reviewed in He et al., 1998), TDP in Silverman's Solution was quantified using Inductively-Coupled Plasma-Optical Elemental Spectroscopy (ICP-OES). Extractants from Steps I-V were analyzed colorimetrically using a BioTek Synery HT multi-Mode microplate reader following protocols outlined in Appendix 4 of Ruttenberg et al. (2009), with the exception of P in Step-II, which was analyzed using a modification of the SepPak method for P-determination in CDB (Suzumura and Koike 1995) (see Appendix to this chapter for modified method).

3.3 Standardization experiments: Design and Procedure.

Efficiency experiments for L-OP: Adapting the work of Laarkamp (2000), the Pre-Extraction method includes a single 2-propanol extraction, followed by multiple B-D extractions. Ultrasonic cell disruption is employed during extraction to effect cell lysis, allowing for liberation and solubilization of intracellular P, and also to disrupt sorptive association of free phospholipids from particulate surfaces (Laarkamp 2000). It was necessary to determine both the number of B-D extractions as well as the optimal length of extraction time required to achieve maximal recovery of L-OP. Laarkamp (2000) found that 4-7 successive B-D extractions were necessary to exhaustively remove L-OP from marine sediments. Because we used cultured phytoplankton cells as our analogue for L-OP (Table 3.1), which we anticipated would be comprised entirely of L-OP, we expected 100% P-solubilization during the Pre-Extraction, and that possibly fewer than 6 successive B-D extractions would be required. In order to maximize OP recovery in a single Pre-Extraction step, the maximum possible volume of extractant permissible was used during each step (13 mL). Extractant volume was limited by the size of the SPEx-Man reaction vessel, which needed to accommodate not only the extractant volume, but insertion of the sonic probe as well, without causing overflow of solution during sonication. Efficiency of the Pre-Extraction for L-OP was determined by subjecting each L-OP analogue to a single 2-propanol extraction, followed by six sequential B-D extractions. Specifically, triplicate 5 mg splits of each plankton analogue phase (Table 3.1) were weighed into SPEx-Man reaction vessels and brought through the Pre-Extraction Step (2-prop extraction + 6 B-D extractions) using 1-minute extraction times. Supernatant of each extraction step was analyzed separately in order to determine the fractional recovery during each successive extraction.

After the optimal number of B-D extractions required for full recovery of OP was determined, the optimal extraction time was evaluated. Laarkamp (2000) used a 10-minute sonication time for B-D lipid-P recovery from marine seabed sediments. A significant drawback to such a lengthy sonication time is that the sample heats up during sonication, necessitating the use of cold-packs to cool the reaction vessel during sonication, which makes the procedure cumbersome and inconvenient. To evaluate whether extraction time could be reduced without sacrificing L-OP recovery, we

compared recovery of L-OP from analogue plankton phases using both 1- and 10-minute sonication times. Specifically, 5 mg splits of the bulk plankton analog phase (Table 3.1) were weighed into replicate reaction vessels and brought through the Pre-Extraction method (2-proponal + 4 B-D extractions) using 1-minute (n=3) and 10-mintue (n=5) sonication times.

Specificity experiments for L-OP: Sequential extraction techniques are operationally defined based on the solubility of target phases in a given extractant. To ensure that the Pre-Extraction method did not interfere with the standardized, operationally defined pools of SEDEX (Ruttenberg 1992; Ruttenberg et al. 2009) we evaluated extent of dissolution of potential sediment matrix phases in the Pre-Extraction method. A suite of naturally occurring minerals, similar to matrix phases used to standardize the original SEDEX method (Table 3.1), was subjected to the Pre-Extraction method followed by the entire SEDEX scheme (Figure 3.1). Matrix minerals artificially loaded with phosphate, as described previously, were assayed, permitting evaluation of matrix phase dissolution during Pre-Extraction, and the extent of release of exchangeable phosphate from non-organic particulate samples during the Pre-Extraction step, and during subsequent SEDEX steps. Specifically, duplicate splits of analogue phases with surface-sorbed phosphate (Table 3.1) were weighed (0.15-0.015 mg) into reaction vessels; optimal weights were determined based on the total P content of each mineral (Table 3.1) to ensure detectable P levels in extractants (data not shown). Samples were then taken through the Pre-Extraction Step (note: 10-min shake time at each Pre-Extraction step was used in this experiment), followed by the full SEDEX scheme.

Matrix effect experiments for L-OP: These experiments were designed to determine whether, subsequent to release of L-OP in natural samples, readsorption of P occurs onto surfaces of other sedimentary phases (hereafter called 'matrix phases') that remain in solid form throughout the Pre-Extraction. Bulk plankton (Table 3.1) was used as the target phase, acting as the 'P-source' material during matrix effect experiments. A split of bulk plankton was placed into a reaction vessel along with one pure matrix phase, and the Pre-Extraction was carried out, followed by the entire SEDEX scheme. By continuing to run the two-phase mixtures through the entire SEDEX scheme we were able to (i) ascertain whether any readsorption that may have occurred during the Pre-

Extraction step was reversed during SEDEX-Step I, which is designed to solubilize loosely-sorbed P (Figure 3.1), and/or whether additional secondarily sorbed P not recovered during SEDEX-Step I might be released in subsequent SEDEX steps. Analogue phases used in this experiments were pure phases of calcite, aragonite, smectite, kaolinite, goethite and ferrihydrite (Table 3.1). None of the matrix phases were expected to dissolve (see later discussion) during the Pre-Extraction step. We note that because the matrix phases are pure minerals, devoid of surface-sorbed phosphate, they are expected to display maximum sorption capacity for solubilized P, and thus may overestimate the potential matrix effect of natural sediments during the Pre-Extraction Step.

Comparison of SEDEX method with and without Pre-Extraction: Plankton analogue phases (Table 3.1) were subjected to the full SPExMan-SEDEX procedure, with and without the Pre-Extraction Step, to determine whether some fraction of OP in the L-OP analogue phases is not solubilized during the Pre-Extraction and, in that case, in which subsequent SEDEX steps this OP would be solubilized. Supernatants from SEDEX-Steps I and IV were analyzed for TDP as well as DIP, using a high-temperature ashing method (Monaghan and Ruttenberg 1999). Step II (CDB) and Step III (Na-acetate) are not amenable to TDP analysis via high-temperature ashing, and these data are unavailable. While bulk plankton is a good analogue for suspended particulate matter in aquatic systems, it is of interest to assay seabed sediments in these experiments in order to evaluate what fraction of sedimentary OP might be solubilized during the Pre-Extraction step, and thus be operationally identified as L-OP. To address this question, we also subjected seabed sediments from two well-studied sites, the Mississippi Delta and Equatorial Atlantic (Ruttenberg et al. 2009), as well as a seabed sample from Kaneʻohe Bay, Hawaiʻi (Briggs et al. 2011), to these standardization experiments.

Combined efficiency-specificity experiments for $CaCO_3$-bound P: To determine the efficiency and specificity of tri-ammonium citrate (TAC) for $CaCO_3$, both $CaCO_3$ and CFA analogue phases (Table 3.1) were subjected to a time-course dissolution experiment. Multiple splits of each analogue phase were weighed (0.3 g) into 50 mL centrifuge tubes and agitated on a shaker table (300 RPM) after addition of TAC (30 mL). Samples were sacrificed serially every hour for 8 hours to determine the dissolution rate, and extent of

dissolution, of each analogue phase. Calcium concentrations determined on supernatant filtrates, analyzed via ICP-OES, were used to determine the efficiency of TAC for dissolving $CaCO_3$, while at the same time evaluating its specificity for $CaCO_3$ over CFA. Phosphorus concentrations were also determined on supernatants via ICP-OES. Because results of these experiments indicated that TAC was not sufficiently specific for $CaCO_3$ over CFA, matrix effect experiments for TAC were not conducted.

3.4 Results and Discussion.

3.4.1 Standardization, Efficiency, and Matrix Experiments for L-OP determination

Filter durability assessment: SEM examination of GH polypropylene (GHP) hydrophilic membrane filters subjected to Pre-Extraction followed by SEDEX showed no evidence of filter degradation resulting from either reagents or physical sonication (data not shown), and thus were confirmed compatible for use with all SEDEX extractants as well as B-D solvents. During the Step V combustion, GHP filters were converted to CO_2, leaving behind no visible residue. PC filters (0.4 μm), successfully used in the 'classical' SEDEX method, dissolved upon exposure to the B-D solvents making them incompatible for the Pre-Extraction method. Thus, if Pre-Extraction is to be employed prior to SEDEX, use of GHP or comparable filters is required. PC filters remain useful for employment of the SEDEX method without Pre-Extraction.

Pre-Extraction efficiency determinations: The recovery of P from L-OP analogues was calculated by normalizing the μmoles of P extracted from each step in the Pre-Extraction Step to the total P extracted from all 7 steps (2-prop + 6 B-D). Between 10-20% of the P was solubilized during the 2-prop extraction, with most of the remaining labile OP (30-50%) recovered in the first B-D extraction (Figure 3.2). After the 4^{th} B-D extraction, recovery efficiency dropped to below 2%. Based on these results, we recommend a final Pre-Extraction Step consisting of a single 2-propanol extraction followed by four successive B-D extractions.

As described previously, 1-minute extractions were employed in the Pre-Extraction efficiency experiment summarized above, with results presented in Figure 3.2. In order to ascertain whether longer extraction times would improve efficiency enough to allow us to reduce the total number of B-D extractions to fewer than 4, and still maintain

Figure 3.2 Phosphorus extracted from each step in the Pre-Extraction method, normalized to the total P extracted from all 7 steps (2-prop + 6 BD). Data is displayed for 3 cultured plankton: dinoflagellates (squares), diatoms (triangles) and green algae (circles), as well as a bulk plankton analog phase (diamonds). See

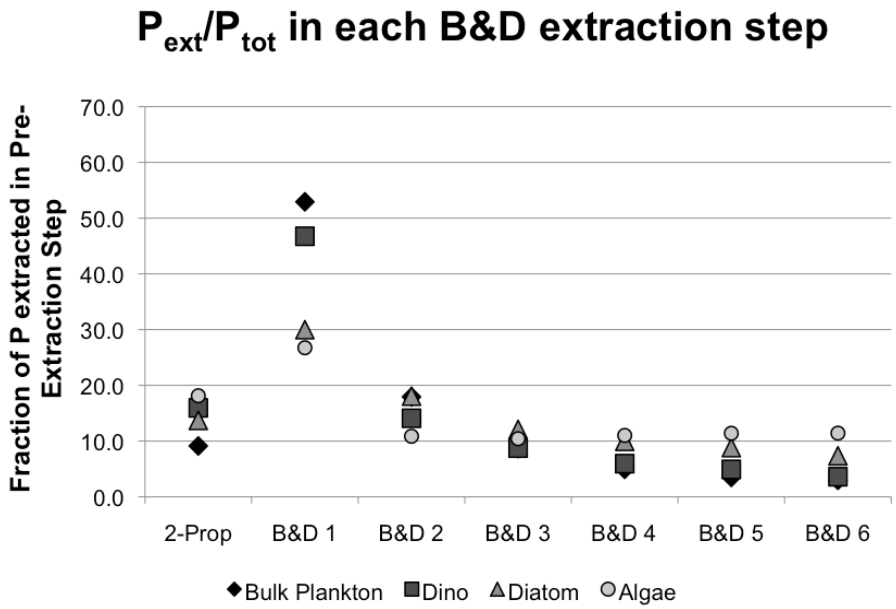

the same level of OP-recovery, we repeated the Pre-Extraction efficiency experiment using both 1- and 10-minute extraction times for each of the 4 B-D extraction steps. The quantity of P extracted during each step was summed to obtain a value for the total quantity of P extracted over the entire Pre-Extraction for each treatment (1- vs. 10-minute extraction) (Figure 3.3). We conclude from these results that the 10-min sonication time does not result in statistically superior P recovery during Pre-Extraction, and thus recommend 1-minute extraction times. Utilizing a 1-min extraction time offers advantages in that the shorter extraction time eliminates the need for cold pack wraps, as outlined by Laarkamp (2000), and it reduces the total time required to complete the Pre-Extraction.

Pre-Extraction specificity evaluation: The possibility of solubilization of P from non-organic sedimentary components (i.e. mineral phases) during the Pre-Extraction is most likely to affect the loosely-sorbed, or exchangeable P (P_{ex}) reservoir (Figure 3.1). The experiment designed to estimate the quantity of exchangeable phosphate that could be released from sediments during the Pre-Extraction Step involved subjecting pure minerals phases that had been loaded with surface-sorbed phosphate to the Pre-Extraction Step followed by the full SEDEX method (Figure 3.1). The fraction of Total P (TP) that

was extracted during the Pre-Extraction was calculated by summing the amount extracted in all 5 extractions (2-prop + 4 B-D extractions) of the Pre-Extraction Step, and normalizing to the quantity of P extracted in the Pre-Extraction plus subsequent SEDEX steps:

% P = (TP in 5 Pre-Ext steps) / (TP in all Pre-Ext plus SEDEX steps) *100 (3.1)

The P_{ex} that was solubilized from matrix mineral phases with surface-sorbed phosphate during the Pre-Extraction step ranged from 0 to 11% of TP, averaging 4 ± 4%, and was highly dependent upon the particular mineral phase onto which the phosphate was surface-sorbed (Table 3.2). For example, <1% of TP associated with aragonite, ferrihydrite, and CFA was solubilized during the Pre-Extraction step, while 6% was released from the goethite and smectite. The largest quantity of TP was released from kaolinite (11%), but it is important to consider the total quantity of P associated with each matrix phase in order to evaluate the impact of fractional solubilization during Pre-Extraction on the accuracy of L-OP determinations. For example, the TP associated with Kaolinite (17.7 ± 0.3 μmol P/ g) is small compared to the P associated with marine plankton (90.5 to 337 μmol P/ g) (Table 3.1). Thus, even if 11% of the P_{ex} associated with Kaolinite is included in the Pre-Extraction supernatant, this should not greatly impact the accuracy of the quantity of P attributed to the L-OP reservoir. Furthermore, it is important to point out that the values that resulted from this experiment likely overestimate of the quantity of P_{ex} released during Pre-Extraction because the minerals assayed were artificially loaded with phosphate. To summarize results of this experiment, P extracted during Pre-Extraction will likely

Figure 3.3 Recovery of OP from the bulk plankton analogue phase in the Pre-Extraction method (2-propanol + 4 B-D) using 1- minute (n=3) and 10-minute (n=5) sonication times. The P extracted was summed over all steps; the standard deviations from replicates are reported as error bars.

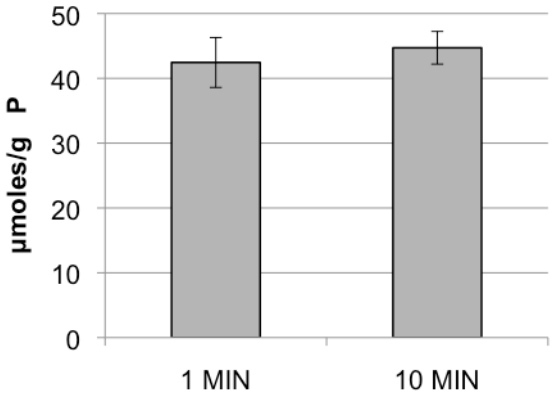

include a small portion of the P_{ex}-pool that is traditionally extracted in Step I of the 'classical' SEDEX method, but will most likely not affect subsequent steps of P extraction.

Table 3.2 Pure minerals with surface-phosphate were taken through the Pre-Extraction method (note: 10 min shaking time at each Pre-Extraction step was used in this experiment), followed by the SEDEX scheme. The percentage of P extracted during the Pre-Extraction method is reported and uncertainty calculated based on duplicate analysis is shown.

Minerals	Percent Dissolution
Aragonite	0.0 ± 0.0%
Smectite	5.8 ± 0.1%
Kaolinite	11.0 ± 2.8%
Geothite	6.2 ± 1.3%
Ferrihydrite	0.3 ± 0.2%
CFA	1.4 ± 0.7%

Evaluation of matrix effects: The goal of the matrix effect experiments was to evaluate the potential for re-adsorption of P released from the target phase (bulk plankton) onto other phases that likely will be present in actual aquatic particulate material. In order to isolate the specific effect of individual matrix phases, we assayed the target phase in isolation with matrix phase. Armed with knowledge of the effect of specific, individual matrix phases on P re-adsorption, one is in a position to evaluate whether a particular natural sediment may exhibit re-adsorption to a greater or lesser extent than is reflected in the experimental results presented here.

To create realistic composite samples that would be reflective of what might be found in natural aquatic systems, we considered the quantity of OP and matrix minerals that might reasonably be present in natural particulate samples. Where possible, we used quantities that reflected average natural conditions, but in some instances, practical considerations about analytical detection limits influenced our decision about quantities used in these experiments. Although the SPExMan-SEDEX method (Ruttenberg et al. 2009) suggests that ~0.1g of sediment is optimal for extraction, since we are using individual components of phases that would make up a bulk sediment, in all cases we used smaller quantities. The quantity of the target phase (bulk plankton) that was weighed into each reaction vessel for the matrix effect experiments was ~20 mg, because this quantity of bulk plankton was necessary to provide enough P such that re-adsorbed P would exceed P-detection limits. We realize that organic P content of typical marine sediments would never be expected to reach 20%; therefore, the matrix effect likely overestimates the re-adsorption of L-OP one might encounter in natural sediments.

The quantity of matrix phase used in each target-matrix phase pair was based upon the relative percentage of that phase in typical marine sediments. The carbonate content of sediments, either as calcite or aragonite, varies widely as a function of depositional environment, ranging from essentially 0 wt% in pelagic red clays to upwards of 90% in nearshore carbonate environments (e.g., Morse and Mackenzie 1990, Kennett 1982, Briggs et al. 2011 – or Chapter 2). Different clay minerals, such as smectite and kaolinite used as matrix phases in these experiments, also occur in widely varying proportions in different sediment environments, but can comprise upwards of 31 to 70% of sediment, respectively, on an organic- and carbonate-free basis (Morse and Mackenzie 1990).We chose to use a quantity of carbonate and clay mineral matrix phases that would be present in a sediment containing 50 wt% carbonate and/or clay on an average bulk sediment basis, and therefore added 0.05 g of pure calcite, aragonite, smectite and kaolinite as matrix phases to be combined with 20 mg of the target L-OP phase in each reaction vessel. (Note: Matrix phases used in these experiments do not have surface-sorbed P associated with them.)

Published values of sediment Fe:Fe-bound P ratios ($Fe:P_{Fe}$) in marine sediments were used as a basis for choosing the quantity of iron mineral matrix phases (goethite and ferrihydrite, Table 3.1) to be used in matrix effect experiments. We wanted to provide sufficient Fe-matrix phase material to ensure ample binding sites for the quantity of P provided by the target L-OP phase. While Slomp et al. (1996) found that $Fe:P_{Fe}$ ratios vary in different sediment environments, these authors suggest that an average ratio of 10 describes most marine sediments. Using an $Fe:P_{Fe}$ ratio of 10 and our choice of optimal target phase mass (≈20 mg), we determined that 3 mg of each Fe mineral would provide adequate number of surface sorption sites to accommodate phosphate solubilized by the bulk plankton target phase during the Pre-Extraction step. Given that if this quantity of Fe mineral were part of a 0.1 g bulk sediment aliquot subjected to SPExMan-SEDEX, this quantity falls within the range of average Fe content of marine sediments, estimated to vary between 2-10 weight percent (Hyacinthe and Van Cappellen 2004; Jensen and Thamdrup 1993). Considering both the average marine sediment Fe content and $Fe:P_{Fe}$ ratio discussed above, we chose to use 5 mg of each pure iron matrix phase, goethite and ferrihydrite, in matrix effect experiments.

Before discussing P re-adsorption onto matrix phases, it is important to evaluate the results shown for the target-phase only samples. Bulk plankton P-recovery was only 72 ± 3% in the Pre-Extraction (Figure 3.4, first blue bars; Figure 3.5). This is perhaps not surprising since, as a bulk surface water particulate sample collected during a plankton tow (Ruttenberg 1992), it may contain some particulate material other than 'pure' phytoplankton. Furthermore, even if the bulk plankton sample is dominated by phytoplankton, if diatoms are present their siliceous tests, which would not be expected to dissolve during the Pre-Extraction, could provide surfaces for P re-adsorption. An additional 13 ± 2% is recovered during Step-I, representing the quantity of secondarily adsorbed P that is recovered by $MgCl_2$, an extractant previously shown to reverse secondary P sorption occurring during SEDEX (Ruttenberg 1992), bringing the total P recovery up to 85 ± 4%. The remainder of the P associated with the bulk plankton

Figure 3.4 Matrix experiment results in which bulk plankton (Table 1) was used as the target phase, or source of labile organic P, and matrix phases were pure mineral analogs: aragonite, calcite, smectite, kaolinite, goethite and ferrihydrite. Each reaction vessel contained 20 mg of bulk plankton and 5-50 mg of the matrix phase. Values are reported as the % of total P extracted in each step. The bulk plankton sample (top bar) did not contain a matrix phase and shows the distribution of P extracted from bulk plankton in each step. Total P (IP + OP) extracted reported for Pre-Extraction and Steps I, IV, and V was analyzed using a high-temperature ashing method (Ruttenberg and Monaghan 1999). Inorganic P (IP) only is reported for Steps II and III.

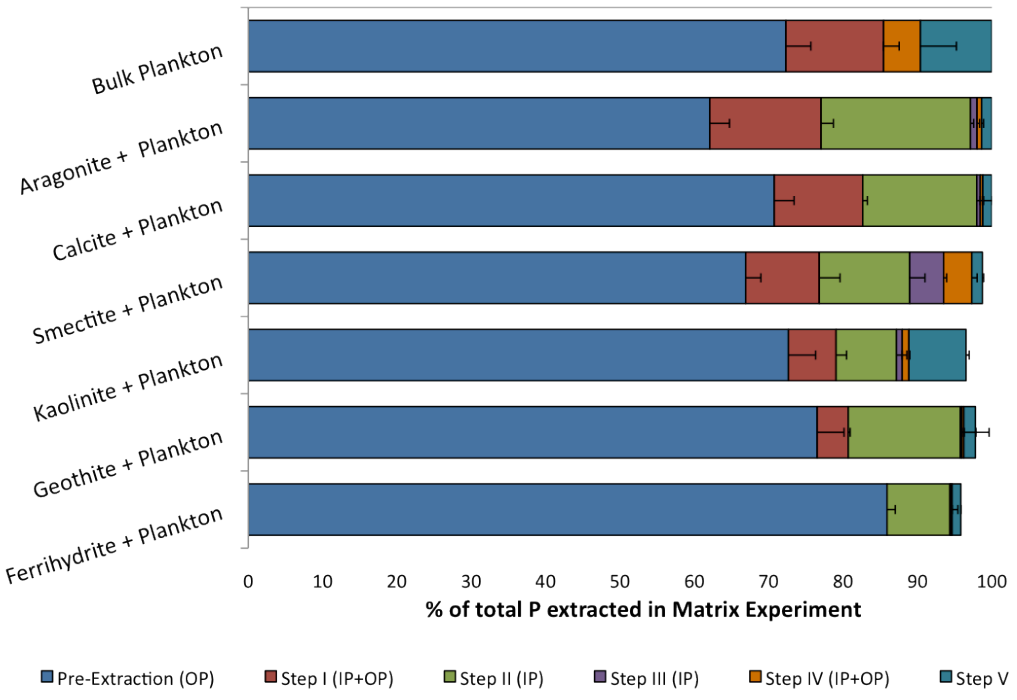

analogue phase is solubilized during SEDEX-Step IV (5 ± 3%) and Step V (10 ± 1%). P recovered in Step V represents a refractory component of organic matter, which may derive from phytoplankton (see discussion of pure plankton recovery, below), but could equally derive from terrestrial organic matter that might have been included in this bulk net-tow sample.

The quantity of P recovered in the Pre-Extraction step from the matrix plus target phase combinations ranged from 62-86% (Figure 3.4); average recovery was 72 ± 3%, which was equivalent to the expected P recovery in the Pre-Extraction step based on the quantity of bulk plankton L-OP (matrix phase alone) (Figure 3.5). The re-adsorption effect was determined as the difference between the P recovery expected (% based on bulk plankton matrix phase) and the actual percentage recovered in the Pre-Extraction step. Re-adsorption effects were most severe for aragonite, (10 ± 4 %) and calcite (5 ± 4%), with undetectable re-adsorption (within the range of uncertainties) occurring onto kaolinite, smectite, and goethite. All recoveries fall within the range observed for the target phase with the exception of ferrihydrite, which displayed higher recoveries of L-OP (86 ± 1%). Recent studies have shown that ferrihydrite can cause surface catalyzed DOP hydrolysis (Baldwin et al. 1995; Bladwin et al. 1996; Ruttenberg and Sulak 2011), thus the higher P recovery from ferrihydrite in the Pre-Extraction step be due to hydrolysis of surface associated OP.

Having observed incomplete recover of L-OP from bulk plankton in the matrix effect experiment, we examined the P recovery in the remaining SEDEX steps in order to evaluate where the un-recovered phytoplankton-associated P might be released (Fig. 3.4). As previously mentioned, P recovered from the bulk plankton analog (no matrix phase present) in the Pre-Extraction plus Step I was 85 ± 4%, which falls well in-line with the recovery of P when matrix phases were present (Figure 3.4). On average, for all matrix experiments, 38% of P associated with phytoplankton was not recoverable in the Pre-Extraction step, but between 4 to 15% of re-adsorbed P was recovered in Step I, bringing the total P recovery from both Pre-Extraction and Step I to 76-87% (Figures 3.4).

The majority of the remaining phytoplanktonic-P was released in Step II for all phases except for smectite, which displayed P release in Steps III and IV (consistent with Ruttenberg, 1992), and Kaolinite, which displayed release in Step V (Figure 3.4).

Figure 3.5 Partitioning of P extracted from bulk plankton, diatoms, dinoflagellates, and green algae analogue phases (Table 1) subjected to the full SEDEX procedure, with and without Pre-Extraction (dark and grey bars, respectively). Total P (IP + OP) extracted reported for Pre-Extraction and Steps I, IV, and V was analyzed using a high-temperature ashing method (Ruttenberg and Monaghan 1999). Inorganic P (IP) only is reported for Steps II and III. The sum of P extraction from Pre-extraction plus Step I is given below the graphic in italics. Values reported adjacent to bars in the bar graph report the percent of total P extracted in each step.

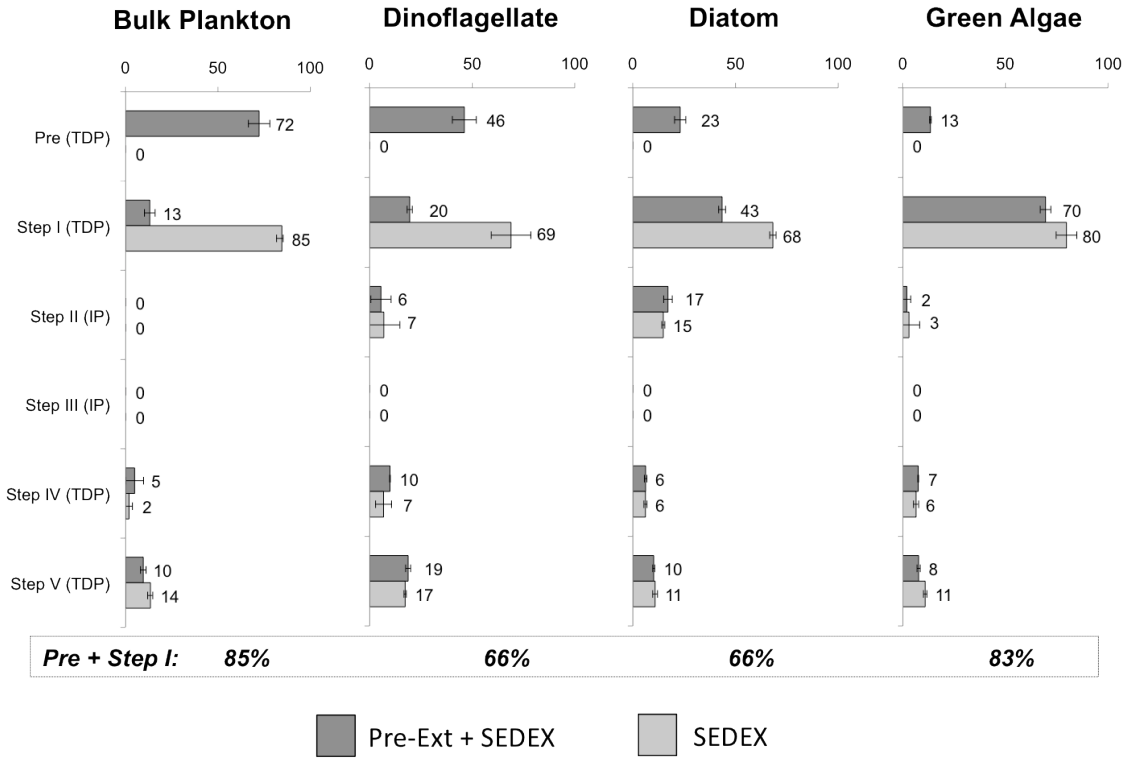

Recovery of the remaining phytoplanktonic-P appears to be influenced by the nature of the specific matrix phase present. For example, secondarily sorbed P may have become irreversibly sorbed onto matrix phases, to be released only when these matrix phases are solubilized; this is likely the case for P sorbed to Fe phases, goethite and ferrihydrite (see Ruttenberg (1992) and Ruttenberg and Sulak (2011) for a discussion of irreversible P sorption onto iron (oxy)hydroxides). In the case of P released from carbonate phases and clays during Step II, however, it is possible that the citrate in the Step-II extractant (CDB, Figure 3.1) effects partial dissolution of the matrix phases; this is particularly likely for the carbonate phases as Ca^{2+} forms stable soluble complexes with citrate (Stumm and Morgan 1981), but may also occur with clays, as Al^{3+} may be partially solubilized via chelation with citrate, as well. Partial solubilization will affect mineral surfaces, and thus may result in collateral solubilization of surface-sorbed P. We note that the fact that P

solubilized from kaolinite in Step V is consistent with results of Ruttenberg (1992), who reported P-recovery from another 1:1 clay, illite, after ashing during Step V, and suggests that solubility of some clay may be enhanced after ashing at high temperatures.

It is important to emphasize that the average recovery in the Pre-Extraction step for all matrix experiments was equivalent to the bulk plankton P recovery in the Pre-Extraction (without matrix phase present), and amounted to an average L-OP recovery of 72%. While some redistribution of the remaining phytoplanktonic-P onto matrix phases occurred via re-adsorption, overall recovery of 72% L-OP indicates that matrix effects do not impede recovery of the bulk of L-OP during the Pre-Extraction step.

3.4.2. Efficiency and specificity of TAC for $CaCO_3$-P.

Maximum $CaCO_3$ dissolution of ~55% was achieved after 8 hours in TAC with a solution:solid (s:s) ratio of 100 (ml:g) (Figure 3.6a). While it is possible that a higher s:s ratio would have enabled higher recoveries, this line of inquiry was not pursued further due to the fact that enough CFA dissolution occurred, even though it never exceeded 7% throughout the 8-hr time course (Figure 3.6a), to render successful separate quantification of $CaCO_3$-P via TAC unlikely. We use data from Ruttenberg (1992), who reported that shells used as $CaCO_3$ and CFA analog phases have associated with them 0.4 wt% and 11.66% P, respectively, to calculate the P yield expected from 55% dissolution of $CaCO_3$ in TAC, and compare this to the quantity of P expected to be released from 7% dissolution of CFA. Utilizing the wt% of P associated with each mineral and the s:s ratio of 100, 5-7 μmole P would be released from $CaCO_3$, while P release from CFA, experiencing only 7% dissolution, would release between 1500-2500 μmole P. Thus, although extent of CFA dissolution is relatively small compared with extent of $CaCO_3$ dissolution (Figure 3.6b), the quantity of P released from just 7% CFA dissolution could be enough to completely swamp any P release that might be expected to occur as a consequence of $CaCO_3$ dissolution.

We caution that the analysis of results from these dissolution experiments assumes that the quantity of $CaCO_3$ and CFA are equivalent in a given sediment sample, which grossly oversimplifies the natural variability in sediment composition that may be encountered in different depositional environments. In some sedimentary environments, the TAC method for separate quantification of $CaCO_3$-P may still be applicable. For example, if CFA concentrations are exceedingly low and $CaCO_3$ content is relatively large, 7% dissolution of CFA may not necessarily mask $CaCO_3$-bound P. Because our work focuses primarily on sediments with measurable quantities of CFA, the TAC method was judged not to be useful in our study, so no further standardization experiments were run with TAC.

3.4.3 Comparison of SEDEX method with and without Pre-Extraction.

Labile organic P (L-OP) analogue phase results: All phytoplankton analogue phases (Table 3.1) were subjected to the full SEDEX procedure, with and without Pre-Extraction, to evaluate the quantity of P liberated in each step. This experiment allows us to determine in which SEDEX-step the L-OP, solubilized from phytoplankton during the Pre-Extraction step, will be released during the 'classical' SEDEX scheme (e.g., SEDEX conducted without a Pre-Extraction step). Also, this test permits an assessment of

Figure 3.6 Results of $CaCO_3$ and CFA (Table 1) dissolution experiments using Triammonium citrate (TAC). (a) Percent yield of Ca^{2+} quantified via ICP-OES analysis. (b) Percent yield of phosphorus calculated utilizing wt% of P associated with $CaCO_3$ and CFA analog phases (0.4 wt% and 11.66% P, respectively; Ruttenberg 1992).

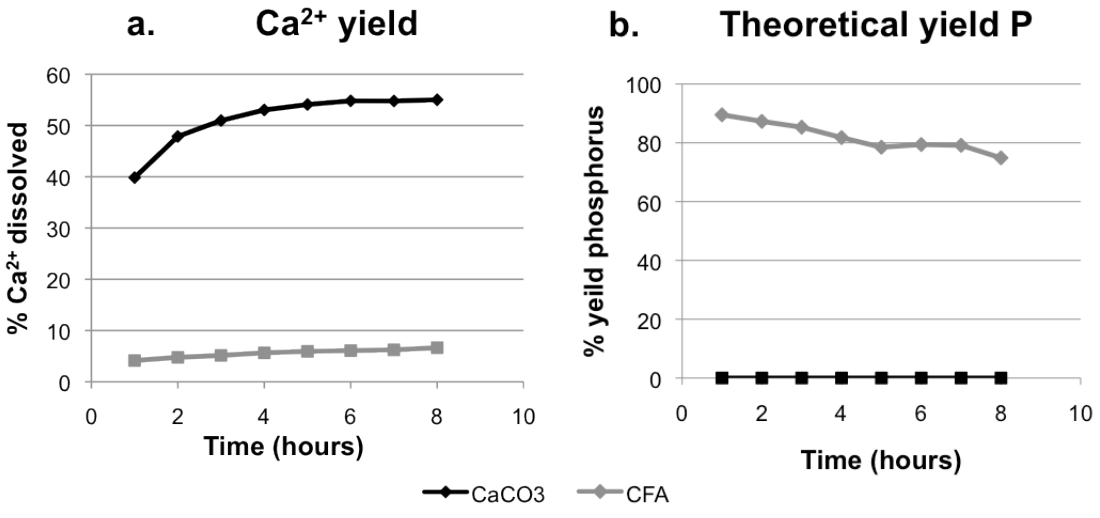

potential variability in L-OP recovery from different types of phytoplankton, including a diatom, a dinoflagellate, and a green alga, as well as the bulk plankton sample, which may be a mixed assemblage of phytoplankton and may contain non-phytoplankton material (as previously discussed).

Pre-Extraction followed by SEDEX: Triplicate splits of phytoplankton analogues (2-5 mg), weighed into SPExMan reaction vessels and subjected to the Pre-Extraction, released between 13 to 72 % of L-OP, with the largest fraction of L-OP released from the bulk phytoplankton analogue (72%) followed by the dinoflagellate (46%), diatom (23%) and the lowest quantity released from the green alga (13%) (Figure 3.5). The quantity of P released during Step I is operationally-defined as loosely-sorbed P (P_{ex}), and represents L-OP released during Pre-Extraction but sorbed onto solid-phase residue remaining after Pre-Extraction. When the quantity of P released during Step I is combined with that released during Pre-Extraction, the total released during Pre-Extraction + Step I is 85% from the bulk plankton, 66% from both the dinoflagellate and diatom, and 83% from the green alga (Fig. 3.5). The dissimilarities between algal taxa in partitioning of L-OP solubility are striking, and reflect either differences in the nature of DOP released during Pre-Extraction, or differences in the nature of the residual solid phase that provides surfaces for secondary P sorption, or both. Despite these differences, however, the bulk of P within these L-OP analogue phases, between 66 and 85% of L-OP, is accounted for by the P solubilized during Pre-Extraction and Step I.

Step V is the only other step where a consistently sizable fraction of P is recovered from all plankton analogue phases. Between 8 and 19% of phytoplankton cellular P are recovered in Step V (Figure 3.5). The fact that this quantity of P was not soluble until after ashing at 550°C suggests that, according to the operationally-defined nature of Step-V-solubilized P, this fraction of cellular phytoplanktonic P is refractory in nature. This surprising result will be discussed further, below. Smaller quantities (≤10%) of P were solubilized from all four L-OP analogue phases in Step IV, no detectable L-OP was released during Step III.

The quantity of P released during Step II, although small, merits some discussion because prior studies have found P extractable from cultured phytoplankton in extractants specific for reactive Fe-oxyhydroxides (Sanudo-Wilhelmy et al. 2004). Sanudo-Wilhelmy

et al. (2004) argued that P is present in phytoplankton as both surface-adsorbed and intra-cellular pools, and this result has been the basis for speculation about the integrity of the Redfield Ratio concept. The amount of P associated with cultured phytoplankton that is solubilized in Step II in our study, and is therefore operationally-defined as P associated with Fe-oxyhydroxides (P_{Fe}), ranges between 2 to 17% (Figure 3.5); no P_{Fe} was solubilized from the field-collected bulk plankton sample in Step II. Our results do not allow us to distinguish between L-OP originally associated with intact phytoplankton cells that was solubilized during the Pre-Extraction and secondarily sorbed onto phase(s) which were subsequently solubilized during Step II, from P_{Fe} that may have formed on surfaces of analog plankton cells during the culturing process. Because only cultured phytoplankton displayed a substantial quantity of P_{Fe}, it is unclear whether such a pool exists in natural phytoplankton populations. At this point, we can only concur with Sanudo-Wilhelmy et al. (2004) that this observation is intriguing, and that the possibility exists that a fraction of P, operationally defined as OP associated with phytoplankton, may not actually be organic in nature. If accurate, this result potentially undermines, to some extent, the valuation of the canonical Redfield Ratio of 106C:16N:1P, given that a portion of operationally-defined 'Redfieldian-P' might be surface sorbed P_{Fe} and not cellular OP.

Phytoplanktonic L-OP extracted in Pre-Extraction and Step I: The quantity of TDP (DIP + DOP) extracted from phytoplankton in SEDEX-Step I, without Pre-Extraction, is statistically equivalent to quantity of P extracted in Pre-Extraction + Step I (Figure 3.7). This result suggests that application of the 'classical' SEDEX method, without Pre-Extraction, will remove the bulk (66-85%) of L-OP prior to subjecting the residual sediments to the remaining SEDEX steps, so that most of the L-OP pool is recoverable in SEDEX-Step I. It is important to note, however, that quantification of the L-OP solubilized during SEDEX-Step I will only occur if this extract is subjected to TDP analysis, so that solubilized DOP will react colorimetrically and thus be detectable by the molybdate blue method (Monaghan and Ruttenberg 1999). If TDP analysis of SEDEX-Step I is not done, our results suggest (Fig. 3.7) that between 30-40% of the L-OP pool will remain undetected, and will be lost from the full accounting of P distribution in the sample.

Figure 3.7 The percentage of TDP (DIP + DOP) extracted in Pre-Extraction + Step I (first bar) from all analog phytoplankton phases, compared to the percentage of TDP extracted in Step I only (second bar). TDP and DIP were analyzed in all supernatants, and the distribution of P between DIP and DOP is shown as follows: Step I-DIP (blue), Step I-DOP (green), and Pre-Extraction TDP (red).

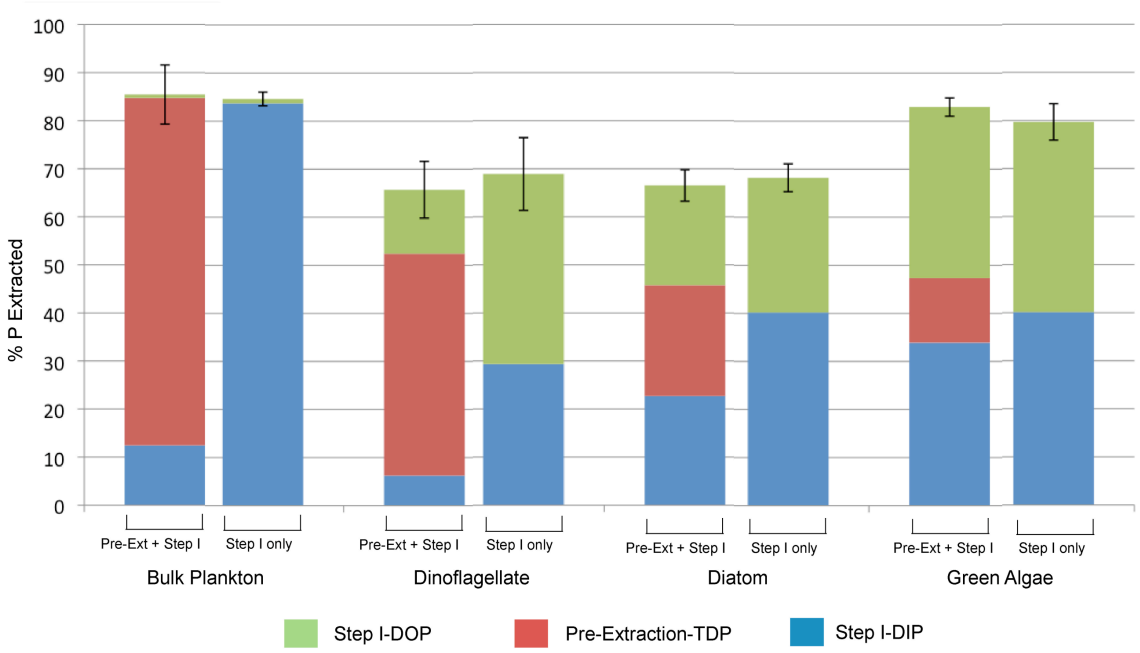

The quantity of DOP recovered from all cultured phytoplankton subjected to Step I but not Pre-Extraction exceeds the quantity of DOP recovered in Step I when Pre-Extraction was conducted (Fig. 3.7), indicating that the Pre-Extraction step recovers a portion of the L-OP pool that would otherwise be solubilized during Step I. Recovery of DIP in Step I when Pre-Extraction is not employed is always greater than the quantity of DIP recovered from Step I when it follows the Pre-Extraction step, suggesting either that hydrolysis of DOP occurs during the Step I extraction, or that P quantified as TDP in the Pre-Extraction solution is a combination of DOP and DIP. This latter could be the case if a portion of the intracellular phytoplanktonic P was phosphate or polyphosphate, as can happen under luxury P consumption conditions (Cembella et al. 1982). We are unable to distinguish between these two possible mechanisms that supply DIP from L-OP analogue phytoplankton phases during extraction, and can only state that it may represent either intracellular inorganic P, or be the result of hydrolysis of reactive DOP that may occur during cell-lysis and extraction.

To summarize, these results suggest that application of the Pre-Extraction method to sediments is not required if the objective is to quantify the combined pool of labile and

Figure 3.8 Comparison of P distributions obtained for marine sediment samples from three depositional environments as determined by the combined Pre-Extraction-SPExMan-SEDEX method (dark grey diamonds), as compared to the SPExMan-SEDEX method without Pre-Extraction (light grey squares). All values are reported in µmoles P g^{-1} sediment. Data for Mississippi Delta and Equatorial Atlantic sediments that were brought through the SPExMan-SEDEX method only are from Ruttenberg et al. (2009).

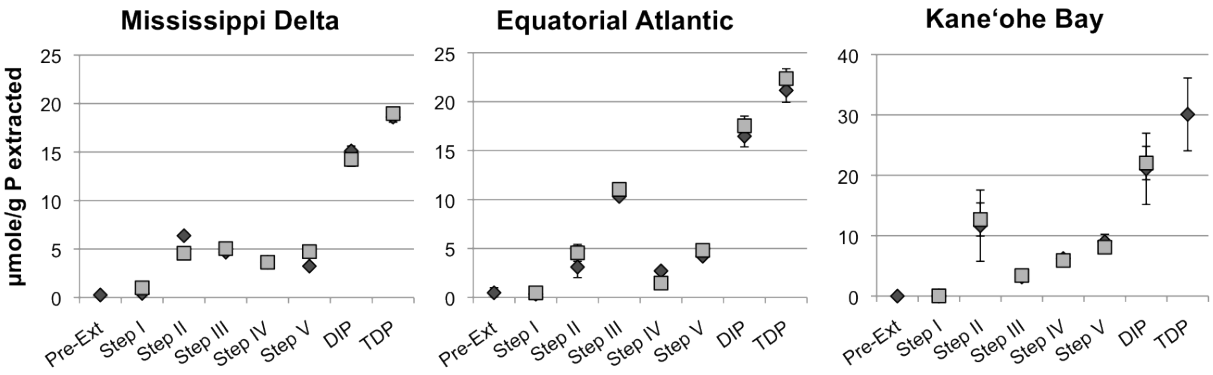

exchangeable P, without differentiating DOP from DIP. If the Step I supernatant is subjected to a TDP analysis, which will convert all DOP to DIP, then the quantity of TDP recovered in Step I will be equivalent to the combined (P_{ex} + L-OP) pool. If, on the other hand, the objective is to separately quantify L-OP, and potentially subject the L-OP pool to other analytical protocols to obtain further details about the nature of this pool (ie. Column chromatography, NMR, or other forms of spectroscopy), the Pre-Extraction step will permit the separate recovery of L-OP for its quantification and further investigation.

Comparison of SEDEX data from seabed sediments with and without Pre-Extraction: Sediment samples subjected to the Pre-Extraction Step did not display sizable quantities of L-OP relative to the quantities of P recovered in subsequent SEDEX steps (Figure 3.8). As a consequence, the concentrations of P recovered from each SEDEX reservoir are similar, to indistinguishable, whether or not the Pre-Extraction step was included (Figure 3.8). The absence of L-OP, as operationally defined by the Pre-Extraction, from seabed sediments from these three distinct depositional environments suggests that the OP reservoir in these surface sediments is relatively refractory. Unless surface sediments are collected immediately after deposition of a crashing phytoplankton bloom, or host a substantial layer of microphtyobenthos, it seems a good assumption that the organic P component of seabed organic matter is relatively refractory. Thus, unless the sediments have had a recent infusion of fresh (and therefore labile) organic matter, it

is probably safe to apply the SEDEX method without Pre-Extraction to seabed sediments, without risk of losing or mis-identifying L-OP, as originally argued in Ruttenberg (1992). Results from extraction of pure phytoplankton analogue phases (Figure 3.5), however, suggest that when analyzing water column suspended material that may be dominated by cellular OP, the Pre-Extraction method is useful for separately quantifying the labile OP pool.

Figure 3.9 The percentage of P extracted from two types of pure DNA (Sigma CAS #9007-49-2; Fisher CAS #BP25141, DNA-1 and DNA-2 respectively) by the Pre-Extraction method, Step I of SEDEX ($MgCl_2$ wash) and a final ashing step. Error bars represent the standard deviation calculated over triplicate analysis of each sample.

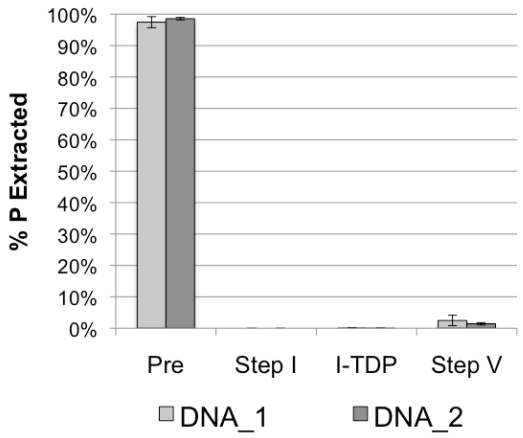

3.4.4 Further insight into 'Refractory phytoplanktonic-P'.

As previously discussed, the Step V recovery of a substantial fraction of OP from phytoplankton analogue phases raises the possibility that a portion of cellular P may, in fact, be refractory in nature. This is an intriguing possibility as it runs counter to our preconceived notions about the nature of cellular OP. In addition, it is tempting to align these results with the often-speculated upon refractory OP pool that could be responsible for the low organic C:P ratios observed in environments characterized by low concentrations of refractory organic matter, such as pelagic and certain deltaic environments (e.g., Ingall and Van Cappellen 1990; Ruttenberg and Goñi 1995). Another possibility is that this apparently refractory OP is an artifact, and may result from failure to solubilize DNA, a highly insoluble molecule that will only dissolve in polar-to-neutral solutions. We considered the possibility that the non-polar nature of the solvents in the B-D reagent might inhibit the solubilization of DNA during Pre-Extraction and subsequent the SEDEX extractions, but that DNA would decompose during muffling at 550°C, and could then be solubilized during Step V.

To test the possibility that L-OP recovered in Step V may result from failure to extract and solubilize cellular DNA in prior steps, two types of DNA (Sigma CAS #9007-

49-2; Fisher CAS #BP25141) were taken through the Pre-Extraction method, Step I of SEDEX ($MgCl_2$ wash), and subjected to a final ashing step equivalent to SEDEX-Step V. The fact that DNA was fully recovered (98-99%) in the Pre-Extraction Step (Figure 3.9) allows us to conclude that the OP that is recovered from phytoplankton analogue phases in SEDEX-Step V, while it remains insoluble during Pre-Extraction, cannot be attributed to failure to solubilize cellular DNA from phytoplankton. Thus, the mystery of the nature of the 'refractory' phytoplanktonic P pool persists, and awaits further work to reveal the nature of this highly refractory OP pool that is rendered soluble only after ashing at high temperature (550°C).

Appendix 3.1 Sep-Pak analysis of SEDEX-Step II (CDB) supernatants for quantification of Fe-bound P.

Step II of SEDEX utilizes a citrate dithionite bicarbonate (CDB) solution to selectively dissolve Fe-bound P. The CDB solution cannot be analyzed via the standard molybedenum blue method due to interferences from citrate with color formation. The butanol extraction method of Watanabe and Olsen (1962) was previously used to separate liberated soluble reactive phosphorus (SRP) from the CDB solution in the Step II of the SEDEX method (Ruttenberg 1992). This analysis yields variable precision, ~10-20% and can sometimes be as poor as 50%. Therefore, finding a new, precise method for the determination of P in Step II extracts was necessary.

We utilized a solid-phase extraction technique by Suzumura and Koike (1995) to replace the Watanbe and Olsen pretreatment of CDB solution. The method works by converting SRP in solution to a 12-molybdophosphric acid (12-MPA), which is adsorbed from the aqueous solution onto a non polar solid-phase cartridge. The 12-MPA is then eluted off the column and analyzed for SRP by the standard molybedenum blue method of Koroleff (1983). Our method employs several modifications to the method outlined by Suzumura and Kioke (1995), which to increase the efficiency of this method, as well as tests the reusability of seppak cartridges.

The sep-pak technique utilizes a Waters© Sep-Pak cartridge packed with polystyrene divinylbenzen (PSDVB). In the original sep-pak manuscript, Suzumura and Koike (1995) utilize a PS-1 cartridge by Waters. This cartridge has since been replaced by a PS-2 cartridge, which we find works with the same efficiency. The cartridge is manufactured by Waters, Japan, but can be ordered through the US Waters Corp (Part # JJAN20151); there is no US manufactured replacement part. The cartridge was equipped with a make-shift reservoir by attaching the seppak cartridge to the barrel of a luer-lok 20cc syringe, which fit snugly together. The cartridge and adapted reservoir were attached to a PTFE manifold stopcock needles (AllTech) on a 24-port SPE glass column processor (JT Baker). The glass rig was connected to a vacuum pump, which allowed simultaneous filtration of multiple samples through the sep-pak columns.

Standard solutions were made (0-150 μM range) using 10 μmol ml^{-1} phosphate stock solution in a CDB matrix. All standards were brought through the procedure

identical to samples. The procedure, as described below, results in a 10-fold dilution therefore final concentration ranges of standards were 1-15 μM (note: the procedure does not have to result in a 10-fold dilution, if you start with 10ml of solution and scale prior to elution, there will be no dilution). Samples from the SEDEX method are typically highly concentrated so the 10-fold dilution works well and eliminates both the production of waste when utilizing larger sample size and dilution prior to analysis. Additionally, diluting the CDB extractant prior to sep-pak recovery of SRP assisted in the complete recovery of liberated P. A 10-fold dilution of CDB samples (or standards) with MQ-DI water (1mL CDB and 9mL MQ-DI) was employed immediately following the recovery of filtrate from Step II in the SEDEX method. The CDB solution is not stable, due to the volatility of dithionite in its aqueous form, thus it is suggested to pretreat and analyze CDB extracts immediately after completion of Step II. CDB extracts that were treated and analyzed several weeks later resulted in slightly lower recovery of SRP (data not shown).

A pretreatment with $FeCl_3$ prevents the interference of citrate with the reduction of the molybdate complex (Lucotte and D'Angeljan). After the 10-fold dilution, samples were reacted with 1% v/v 1M $FeCl_3$ solution (initial color is a dark yellow). Analytical grade $FeCl_3$ has a 0.01% maximum PO_4 blank. If larger volumes of $FeCl_3$ are used the P blank from $FeCl_3$ can result in a final P signal that masks the signal of SRP solubilized in CDB. After the addition of $FeCl_3$, samples are allowed to react overnight (final color is a pale light yellow).

The next morning samples were mixed with acid-molybdenum solution (Suzumura and Koike 1995) at a volume ratio of 3:1 to convert SRP to 12-MPA. Prior to running samples through the cartridge, the sep-pak was prepped and washed according to Suzumura and Koike (1995) using 3 mL of methanol and 5 mL of 1N sulfuric acid. After the sample was passed through the cartridge a yellow plug appeared, indicating retention of the 12-MPA complex. Cartridge and reservoir were then washed with 5 ml of 1N sulfuric acid to remove all residual citrate dithionite. The 12-MPA was eluted off the column and collected using 5 ml of 0.5M ammonium solution (yellow plug disappears). An additional 3 mL of 1N sulfuric acid and 2 ml of MQ-DIW was passed through the column and collected with the 5 ml of 0.5M ammonium solution, bringing the solution to

Appendix Figure 3.1 Reusability test on the Sep-Pak cartridges to examine carry over on each column. Standards were run through the same Sep-Pak cartridge 5 times; all standards were within 5% error.

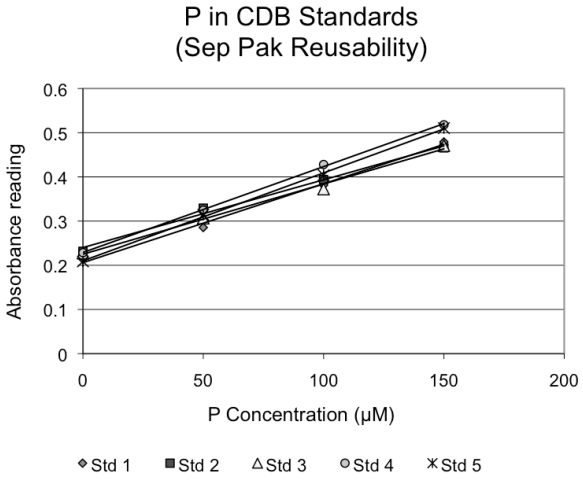

a final volume of 10 ml at pH 1. Samples were then analyzed using the standard molybdenum blue method with a BioTek Synergy HT Multi-Mode Microplate Reader (Grasshoff, 1972).

Cartridges are reused multiple times during analysis. A simple reusability test was conducted to examine carry over on each column. We ran standards through the same sep-pak cartridge 5 times and found all standards were within 5% error. This experiment demonstrates the high reproducibility of this method and also suggests no carry over during re-use of the cartridge even at high (150 µM P) concentrations (Appendix Figure 3.1).

Appendix-3.2 Miscellaneous analytical details regarding Pre-Extraction.

We were surprised and perplexed that during a first attempt to test the specificity of the Pre-Extraction for L-OP large quantities of P were extracted from each pre-sorbed mineral phase with the B-D solvent mix. Closer examination revealed that the B-D reagent used in this first test was extremely acidic (pH~2). We learned that chloroform ($CHCl_3$) degrades to hydrochloric acid over time, and it turned out that the particular bottle of chloroform we initially used to make up our B-D reagent had decomposed substantially and, as a result, had become acidic. When new, non-degraded chloroform is used, the final pH of the B-D solution should be between pH 7 to pH 8.5. Thus, prior to using the B-D reagent, pH should be measured, to guard against employing an inadvertently acidic Pre-Extraction solution, which will actively dissolve non-organic, mineral-P that will normally comprise the operationally defined pools of SEDEX-Steps I-IV.

Acknowledgments

Mashiro Suzumura supplied important suggestions that guided initial stages of method development for the $CaCO_3$ extraction, as well as information and assistance with the Sep-Pak method, which we gratefully acknowledge. Sonya Dyhrman and Sheehan Haley at WHOI provided cell cultures, which we gratefully acknowledge. We would like to thank Marcie Grabowski and Kathryn MacDonald for laboratory assistance and James Cowen for access to the SEM. This work was funded grant/cooperative agreement from the National Science Foundation. The views expressed herein are those of the authors and do not necessarily reflect the views of NSF or any of its sub-agencies. This is SOEST contribution #xxxx.

Chapter 4

Linking source, abundance and lability of sedimentary organic matter to remineralization efficiency

with A.E. Ricardo, K.C. Ruttenberg, B.T. Glazer

Abstract

This study systematically relates how variations in source (and therefore lability) of organic matter (OM) affects rates of OM degradation in marine sediments. Molar OC:TN:OP ratios are used in tandem with carbon isotopic values to constrain sources of OM to sediments. OC:TN ratios are a weaker indicator of OM source than OC:OP ratios, because: (i) the more restricted dynamic range of OC:TN ratios prevents clear distinction of terrestrial- from marine-derived OM, and (ii) post-depositional changes in OC:TN ratios occur during diagenesis, obscuring the source signature of initially deposited OM. Whole sediment cores collected along a shore-to-bay transect were embedded with voltammetric microelectrodes and incubated in the laboratory. Rates of O_2 consumption, H_2S production, and NH_4^+ accumulation in porewaters were quantified as proxies for microbial OM remineralization. Higher remineralization rates were observed at sites located farthest from the shore where sediments were characterized by more labile, marine-dominated OM; progressively slower remineralization rates were observed as the fraction of terrestrial (more refractory) OM increased in sites proximal to the shore. Although larger quantities of OM were deposited at the most landward site, resulting in larger quantities of regenerated inorganic nutrients per unit time and greater benthic nutrient fluxes, specific remineralization rates were lower at this site. This contrast makes clear the importance of distinguishing between quantity versus quality of OM when assessing remineralization rates.

4.1 Introduction

Organic matter (OM) in coastal aquatic sediments derives from marine sources, such as seagrasses, micro- or macroalgae and phytoplankton, as well as terrestrial sources that are principally delivered by rivers. In areas where mangrove forests are present, mangrove litter can contribute OM to coastal sediments, as well. If OM is not respired within the water column or physically transported out of the system, it settles to the sediment, where it is subjected to degradation and chemical alteration by the benthic community. A portion of degraded OM may be recycled into the overlying water as dissolved organic matter or inorganic nutrients, the products of OM remineralization. The residual material is incorporated into sediments, where it can be further degraded during burial. Most of the organic carbon (94%) preserved in marine sediments is buried in continental margin sediments (Berner 1982; Hedges and Keil 1995). Therefore, understanding the sources, lability and subsequent preservation of OM in coastal sediments is essential to understanding carbon cycling in the global ocean.

Marine derived OM is generally more labile than its refractory, terrestrial counterpart (Aller et al. 1996; Cowie and Hedges 1992). The principle tools for distinguishing marine versus terrestrial OM are elemental ratios and isotopic composition. While marine phytoplankton have a mean molar organic carbon to total nitrogen to organic phosphorus (OC:TN:OP) ratio of 106:16:1 (Redfield et al. 1963), terrestrial, vascular plants have characteristic OC:OP up to or exceeding 800, and OC:TN ratios ranging up to or exceeding 1000 (Likens et al. 1981). Bulk sediment stable isotope signatures provide an additional, independent tool for the identification of OM sources to sediments (e.g., Hedges and Parker, 1976, as cited by Goñi et al. 1997). Organic compounds derived from marine OM are enriched in ^{15}N and ^{13}C relative to compounds originating as terrestrial OM (Gearing et al. 1977; Goñi et al. 1998; Ogrinc et al. 2005). Isotopic composition is a robust tracer of OM source because isotopic fractionation during digenesis of OM appears to be small, typically less than 2% (Meyers 1997).

OM in surface sediments is metabolically degraded through a complex series of microbial respiratory pathways (e.g., Froelich et al 1979; Burdige 2006). The quality and quantity of OM deposited in coastal sediments will determine rates of OM respiration.

Complete characterization of OM remineralization rates is hindered by our inability to directly measure all of the oxidation pathways in marine sediments (Canfield et al. 1993; Kostka et al. 1999; Thamdrup and Canfield 1996). Due to these constraints, characterization and direct quantification of the dominant microbial OM respiration pathways is often incomplete, and relies heavily on thermodynamic modeling (Nedwell et al. 1993; Rysgaard et al. 1996). An alternative approach to the separate quantification of individual metabolic pathways is to estimate total rates of OM remineralization via changes in oxidant concentrations and the products of OM remineralization (e.g., Canfield et al. 1993). We adopt this latter approach in the present study.

The purpose of this study was to systematically relate how variations in source (and therefore lability) of OM affect rates of OM degradation in marine sediments. Whole sediment cores embedded with voltammetric microelectrodes were incubated in the laboratory and rates of O_2 consumption, H_2S production, and NH_4^+ accumulation were quantified as proxies for microbial OM remineralization. Solid-state Au/Hg glass voltammetric microelectrodes used in this study are a unique tool for estimating sediment redox conditions, as they can simultaneously measure multiple dissolved species, such as O_2 and H_2S (e.g., Luther III et al. 2008 for review). In order to capture a gradient in OM sources, sediment cores for our incubation study were collected along a terrestrial-to-marine gradient from sites located in a protected coastal marine embayment in Kane‘ohe Bay, Oahu, Hawai‘i. We utilize sediment molar OC:TN:OP ratios in tandem with bulk sediment carbon isotopic values to constrain sources of OM to sediments from each site. This multi-tracer approach allows tighter constraints to be placed on the source of OM to coastal sediments than either parameter alone (Middelburg and Nieuwenhuize 1998; Ruttenberg and Goñi 1997a; Ruttenberg and Goñi 1997b). A component of our study included an examination of the effects of diagenesis on the preservation of source signatures of terrestrial and marine OM. Combining estimates of the efficiency of OM remineralization with an analysis of OM sources to depositional environments along a land-to-sea gradient enables us to link the remineralization efficiency directly to OM source, and thus provides insight into how OM source can impact preservation of organic carbon in marine sediments.

4.2 Study Site

Figure 4.1 Aerial photograph of He‘eia Fishpond with study sites marked as white boxes.

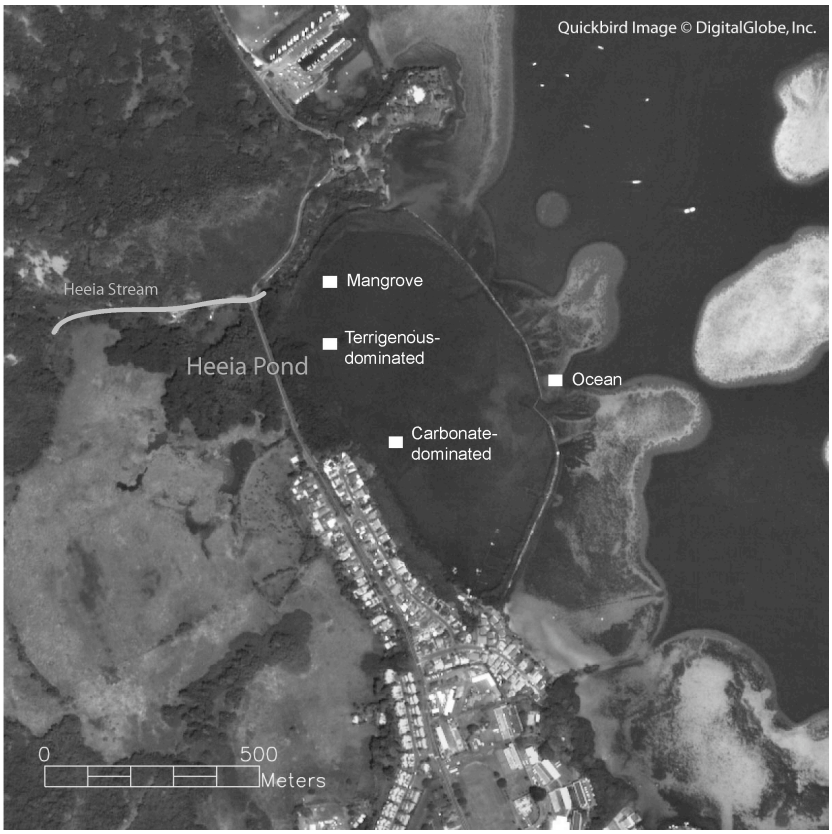

Sediment push cores were collected along a shore-to-bay transect in He‘eia Fishpond, an 88-acre coastal pond located on the eastern side of Oahu, adjacent to Kane‘ohe Bay at the land-sea boundary of the He‘eia watershed (Figure 4.1). The fishpond is a low-energy, shallow coastal system influenced by an influx of both riverine freshwater and seawater from Kane‘ohe Bay, and is ringed by a mangrove forest along its terrestrial periphery. Water flow into and out of the pond is controlled by gates, which are typically left open, rendering the pond analogous to a large mesocosm embedded in a natural coastal environment, making it an ideal site for coastal biogeochemical studies (Young 2011).

In order to study sediments characterized by distinct OM sources and redox conditions, four depositional environments were sampled along a transect extending from the shoreline to progressively more marine-dominated sites. These sites are hereafter defined as: i) Mangrove (collected under the mangrove canopy); ii) Terrigenous-Dominated (collected from a location proximal to riverine input); iii) Carbonate-Dominated (collected from a location distal to riverine input); and iv) Ocean (collected outside He‘eia Fishpond, proximal to the coral reef in Kane‘ohe bay; Figure 4.1).

4.3 Methods

Sample Collection: Two sediment push cores were taken at each site along the terrestrial-to-marine transect. One core was collected for sediment sectioning and porewater extraction and a second core for laboratory incubation experiments. The mangrove and terrigenous-dominated sites were sampled and incubations were initiated on 17 April 2008; four days later the experiment was repeated at the carbonate-dominated and ocean sites. Weather patterns remained constant during this 4-day sampling period, and all cores were collected within the same tidal regime. Thus, cores from all 4 study sites were collected under similar initial physical conditions. Immediately after collection, cores were placed in a bucket of ice to reduce metabolic activity, and covered to inhibit photosynthetic activity during transport to the laboratory.

Tissue samples were collected from terrestrial and aquatic plants that are likely sources of OM to He'eia Fishpond, including mangroves and macroalgae. A surface-water plankton tow (100 μm mesh) was conducted from a small boat, both inside the fishpond and outside, in Kane'ohe Bay. Plankton samples and plant tissues were freeze-dried and analyzed for elemental and isotopic composition to characterize end member sources of OM to the study site.

Core processing and analysis: Cores from each site used to determine initial conditions were sectioned at 0.25 to 1 cm intervals under an inert (N_2) atmosphere to prevent oxidation artifacts (Bray et al. 1973). Porewater was separated from bulk sediment via centrifugation. In order to maximize porewater collection in sandy sediments, we adapted Whatman VectaSpin 20 ® centrifuge tubes that allow filtration during centrifugation by replacing the manufacturer installed polypropylene filter with a coarse (1.2 μm) GF/F filter. The coarse GF/F filter allowed maximum recovery of sediment porewater, which was subsequently filtered using a 0.4 μm Pall Life Sciences GHP acrodisc ® filters. Filtered porewater was split into two subsamples: a frozen, untreated split and a refrigerated-acidified split. Samples were analyzed for dissolved inorganic phosphate (DIP) and ammonium (NH_4^+) using established colorimetric protocols on a BioTek Synergy HT Multi-Mode Microplate Reader (Grasshoff et al. 1983); all reported data have a 2% standard error associated with them. Colorimetric detection on small porewater sample volumes (300 μL) can be conducted using the

microplate reader, which allowed for the analysis of multiple dissolved constituents on a single porewater interval, despite the small volumes of porewater collected from each interval. We used Nunc 96-well Optical Bottom Plates ®, which have a 1-cm path length, comparable to that of standard spectrophotometric detection. However, analyses conducted on the plate reader have a slightly higher detection limit than traditional spectrophotometers (0.2 μM for PO_4^{3-} and NH_4^+).

After removal of porewater, sectioned sediments were frozen under an inert atmosphere until freeze-dried under vacuum to prevent oxidation artifacts (Bray et al. 1973; Krall et al. 2009). Sediments were ground with an agate mortar and pestle, sieved (<125 μm) and stored in a sealed vessel prior to analysis. Inorganic sedimentary phosphorus (IP) was determined utilizing acid hydrolysis and total sedimentary phosphorus (TP) was determined using the high-temperature ashing/hydrolysis method of Aspila et al. (1976). Organic phosphorus (OP) was estimated as the difference between TP and IP. Total carbon (TC), organic carbon (OC), inorganic carbon (IC), and total nitrogen (TN), as well as carbon and nitrogen isotope values ($\delta^{13}C$ an $\delta^{15}N$, respectively), were determined using a combined coulometric-elemental analyzer-mass spectrometry method adapted for high carbonate sediments (Briggs 2011). Samples were analyzed for carbon and nitrogen at the Isotope Biogeochemistry Laboratory at the University of Hawai‘i, Manoa. Carbon and nitrogen isotopic values are reported using conventional δ-notation with respect to VPDB and atmospheric N_2, respectively.

Incubation set-up: Sediment cores were incubated in the dark for 3 days with constant stirring of the overlying water. The net O_2 consumption and H_2S production were measured using electrochemical analysis of porewater throughout the incubation experiment. Solid-state Au/Hg glass microelectrodes were custom fabricated by sealing a 0.1 mm diameter gold wire into drawn glass tubing and plating mercury on the polished gold surface (Brendel and Luther 1995). Prior to use, electrodes were calibrated using a suite of laboratory standardization methods (e.g. Luther III et al. 2008). For each incubation experiment we operated two voltammetric analyzers (Analytical Instrument Systems, Inc. Model DLK 100a), which utilized a standard three-electrode cell and multiplexed 4 replicate working electrodes in each incubated core. A programmable scan sequence was used to switch between microelectrodes at each depth. Scans were

programmed in a 7.5 min sequence, resulting in a total of four scans per electrode every 7.5 minutes for 3 days.

Each core had one counter and one reference electrode positioned in the overlying water and four working Au/Hg microelectrodes positioned at fixed depths relative to the sediment-water interface (SWI): 2 cm above the SWI, at the SWI, 6 cm below the SWI, and 13 cm below the SWI (Figure 4.2). The depth of each microelectrode was selected based on knowledge of likely positions of redox transition zones from prior work. The overlying water and SWI electrodes were placed in initially oxic regions, the 6 cm electrode was placed in the suboxic zone and the deepest electrode was placed below the suboxic zone (e.g., in anoxic sediments) to capture hydrogen sulfide buildup resulting from sulfate reduction. Changes in detectable concentrations of O_2 and H_2S were measured at each depth throughout the three-day incubation experiment. At the end of the incubation experiment, the sediment core was sectioned and analyzed for solid phase and porewater constituents following the procedures outlined previously.

Figure 4.2 Incubation setup and schematic. Microelectrodes are attached to the micromanipulator and lowered into paired sediment cores. Each core had one counter and one reference electrode positioned in the overlying water and four working Au/Hg microelectrodes positioned at fixed depths relative to the sediment-water interface (SWI) attached to a voltammetric analyzer. Electrodes were placed 2 cm above the SWI, at the SWI, 6 cm below the SWI, and 13 cm below the SWI.

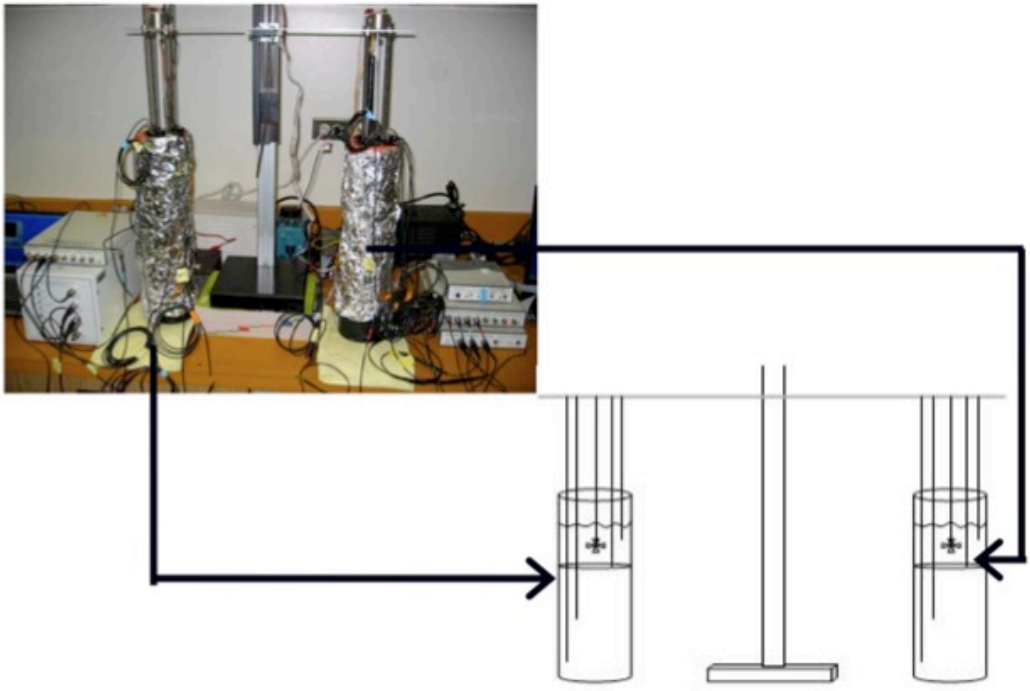

4.4 Estimation of Mineralization Efficiency

Conceptual Framework: The spatial distribution of redox reactive species in marine sediments is dictated by the dominant microbial respiratory pathways employed to oxidize organic carbon at any given point in the sediment, through the reduction of inorganic electron acceptors (i.e., O_2, NO_3^-, oxides of Mn and Fe, and SO_4^{2-}) (Thamdrup and Canfield 1996). For the purposes of this paper we will refer to redox zonations by the classical terms: oxic (the zone with detectable O_2), suboxic (the zone with no detectable O_2 or H_2S), and anoxic (the zone with detectable H_2S from sulfate reduction). We recognize that broadly applying this classification scheme may lead to confusion due to the overlap of metabolic processes within each designated zone (Canfield and Thamdrup 2009); however, because this study examines total combined OM remineralization rates via several metabolic pathways, our adherence to this classical classification of redox zonations should cause no confusion.

OM decomposition rates were estimated via two approaches. The first approach was to measure and calculate rates of O_2 consumption and H_2S production using microelectrodes positioned at the sediment-water interface and at 13 cm within each sediment core, respectively. O_2 is the terminal electron acceptor in respiration pathways, thus rates of O_2 consumption can be utilized to represent the integrated rates of OM oxidation in oxic and suboxic sediment layers. In other words, O_2 is utilized (i) directly in heterotrophic respiration of OM and (ii) as an oxidant for the products of anaerobic OM oxidation by other pathways (i.e., NH_4^+, H_2S, Fe^{2+} and Mn^{2+}); therefore, O_2 consumption rates are directly proportional to total OM oxidation by both aerobic and anaerobic pathways in the oxic and suboxic redox zones (Canfield et al. 1993; Jahnke et al. 2005). Sulfate reduction rates in the anoxic zone of sediments can be estimated by quantifying the production of H_2S, a product of sulfate reduction. Specific rates of H_2S production provide a minimum estimate of OM remineralization via sulfate reduction because abiotic reactions, such as secondary re-oxidation of sulfide or reactions with reduced iron that consume H_2S, were not constrained. Nevertheless, differences in H_2S production rates between sites allowed us to evaluate the impact of organic matter source on mineralization rates at depth in sediment cores from each location.

The second approach used to estimate OM decomposition rates utilized the buildup of porewater NH_4^+, a product of OM remineralization. Porewater profiles of NH_4^+ from pre- and post-incubation sediment cores were integrated and the differences between the integrated profiles were used to estimate rates of NH_4^+ accumulation. This approach provides a minimum estimate of NH_4^+ production from organic matter remineralization over the course of the incubation. In addition to integrating whole sediment core accumulation of NH_4^+, we calculated differences in the diffusional benthic efflux of NH_4^+ from the porewater gradient exhibited in pre- and post-incubation porewater NH_4^+ profiles. Measuring the buildup of inorganic nutrients such as NH_4^+, and the subsequent diffusional fluxes of inorganic nutrients, does not inform us about specific metabolic pathways; however rates calculated this way can be used to compare total OM oxidation rates in different sedimentary environments (Jahnke et al. 2005).

Rates of O_2 consumption, H_2S production, and NH_4^+ accumulation, calculated using the assumptions outlined above, were normalized to the quantity of OM available for remineralization at each site. We define the normalized, absolute rate per mole of OM as the 'specific rate' of remineralization. By normalizing to the quantity of OM, we can directly compare rates (per mole of OM) at each site, and thus remove the effect that quantity of OM has on bulk rates of oxidant consumption or metabolite build-up. The specific rates are thus characteristic of lability of the bulk OM at each location, and reflect the different mixture of terrestrial and marine organic matter present. For instance, although the total rate of NH_4^+ accumulation (not normalized to OM) in the mangrove site is greater than that observed at the ocean site, after normalizing to the quantity of OM at each site, it is clear that the absolute rate per mole of OM (e.g., the specific rate of remineralization) is lower at the mangrove site than at the ocean site. Thus, we will report specific rates at each location, so that we can evaluate relative differences in the efficiency OM remineralization (which is directly related to the inherent lability of the bulk OM in sediments) at each site.

Calculations: Microelectrode detection of O_2 in surface sediments and H_2S at depth within sediment cores was used to calculate specific rates of O_2 consumption and H_2S production according to equation 4.4 (given for O_2 consumption):

$$O_2 \text{ consumption} = (\Delta [O_2]_{SWI}) * (\varphi) * (t)^{-1} * ([OC]_{PRE})^{-1} \quad (4.1)$$

where $\Delta [O_2]_{SWI}$ is the change in oxygen concentration measured at the electrode positioned at the SWI, $[OC]_{PRE}$ is the concentration of organic carbon at the depth of electrode placement in the pre-incubation core (e.g., the SWI), t is the time over which consumption occurred, and φ is porosity.

Matlab Curve Fitting Toolbox™ was used to integrate profiles of NH_4^+ and OC from pre- and post-incubation sediment cores using an integrated smoothing spline. The integrated areas under the curves were used to determine the standing crop (μmole cm^{-2}) of NH_4^+ and OC in pre- and post-incubation cores using the following equations:

$$\text{Standing crop of } NH_4^+ = (\text{Integrated } [NH_4^+]) * (\varphi) * (z) \quad (4.2)$$

$$\text{Standing crop of OC} = (\text{Integrated [OC]}) * (1 - \varphi) * (z) \quad (4.3)$$

where z is the depth over which the sediment profile was integrated (e.g., see Ruttenberg and Berner 1993). Pre- and post-incubation standing crop values were then used to determine specific rates of NH_4^+ accumulation according to equation 4.4:

$$NH_4^+ \text{ accumulation} = (\Delta NH_4^+ \text{ standing crop}) * (t)^{-1} * (\text{OC standing crop})_{PRE}^{-1} \quad (4.4)$$

where t is the time interval between pre- and post-incubation cores (72 hours). Dividing by the standing crop of OC allows calculation of specific rates of NH_4^+ accumulation.

The standing crop of NH_4^+, determined using whole-core profiles of incubated sediment cores, represents a balance between biotic and abiotic production and consumption pathways. Because consumption pathways were not quantified in this study, the specific rates reported are considered minimum estimates of microbial OM decomposition. Nevertheless, these minimum estimates provide insight into the relative OM liability and therefore the ease of OM remineralization at each study site (see Discussion).

Sediment porewater NH_4^+ profiles were used to estimate the diffusional flux of NH_4^+ across the sediment-water interface using Fick's first law of diffusion.

$$J_{sed} = -(\varphi) * (D_{sed}) * (\partial C/\partial x) \quad (4.5)$$

where J_{sed} is the diffusional flux, D_{sed} is the whole sediment diffusion coefficient and $\partial C/\partial x$ is the changes in concentration over depth calculated from porewater profiles. The whole sediment diffusional constant (D_{sed}) was estimated using sediment tortuosity (calculated using the porosity of sediments at each study site) and a molecular diffusional constant for seawater for each analyte (see Boudreau 1997 for equations and average diffusion coefficient values). The D_{sed} value of NH_4^+ calculated for this study was 1.85e-9. The $\partial C/\partial x$ gradient used in these calculations is defined by the difference between the peak concentration of porewater NH_4^+ at depth and the NH_4^+ concentration in the overlying water.

4.5 Results

End member OM source compositions, plotted as property-property box plots, are consistent with previously published values for mangrove and plankton end member tissues (Table 4.1; Figure 4.3). Molar OC:TN:OP ratios and $\delta^{13}C$ values of bulk sediments from pre- and post-incubation cores, plotted in property-property plots (Figure 4.4a and 4.4b), display a transition from lighter $\delta^{13}C$ values (-27 to -22‰), typical of terrestrial OM in mangrove and terrestrially-dominated sites, to heavier marine-like $\delta^{13}C$ values (-16 to -11‰) in carbonate-dominated and ocean sites. OC:OP values drop from high ratios at sites dominated by terrestrial OM, to low ratios in the sites dominated by marine OM; OC:TN ratios do not display a similarly systematic trend along the transect. Open-symbols represent sediment samples from pre-incubation cores; closed symbols represent post-incubation sediment cores that have undergone early diagenetic transformation. Post-incubation samples from the terrigenous-, carbonate-dominated, and ocean sites display lower OC:TN ratios relative to pre-incubation samples (Figure 4.4b); no systematic alteration in OC:OP ratios is observed (Figure 4.4a). Post-incubation samples from the terrigenous-dominated site display a clear shift toward less negative $\delta^{13}C$ values. Ocean and mangrove sites also display a shift to less negative values after the incubation.